HYDRODYNAMIC INTERACTION AND MOORING ANALYSIS FOR OFFLOADING BETWEEN FPSO AND LNG SHUTTLE TANKER

Master Thesis

RATNA NITA PERWITASARI

4/7/2010

NORWEGIAN UNIVERSITY OF SCIENCE AND TECHNOLOGY

PREFACE

This report has been carried out at Department of Marine Technology, Faculty of Engineering Science and Technology at Norwegian University of Science and Technology (NTNU) during the period of January to June 2010.

My gratitude for my supervisor, Prof. Jan Aarness for valuable guidance, advices and discussion. I also want to thank to Einar Bernt Glomnes for help me with SIMO. And special thanks to Sevan Marine ASA that gave me this topic.

I would like to express my grateful for Abdillah Suyuthi for pleasant discussion during my study in NTNU and also for my family and Indra that always give me great motivation. And finally, my gratitude for all parties who have supported me during finishing my study.

TABLE OF CONTENTS

LIST OF SYMBOLS

Φ	Total velocity potential
$\boldsymbol{\eta}$	Incident wave
η	Rigid body motion displacement
$\dot{\eta}$	Rigid body motion velocity
$\dot{\eta}$	Rigid body motion aceleration
ω	Angular wave frequency
$\boldsymbol{i}$	Vector denotation, x-direction
$\boldsymbol{j}$	Vector denotation, y-direction
$\boldsymbol{k}$	Vector denotation, z-direction
k	wave number
ϕ_z	Linearized wave potential velocity
ϕ_0	Incident wave potential velocity
ϕ_R	Radiation potential velocity
ϕ_D	Difraction potential velocity
C	Generalized damping matrix
M	Generalized mass matrix
v	Fluid velocity
a	Fluid acceleration
N	Number of body
n	Normal vector
ρ	Mass density of sea water
p	Pressure fluid
$\vec{F}$	Force over the body

LIST OF PICTURES

LIST OF TABLES

CHAPTER I INTRODUCTION

1.1. Background

Floating structure becomes widely developed in oil and gas industry. Floating Production Storage and Offloading (FPSO) is an integrated structure with ability to move and relocate after the operation complete. In North Sea, there are more than twenty units of FPSO have been installed[1]. The advantage of using FPSO is the cost effectively when it is used on deep sea development or marginal field[2]. The reason is that the huge capacity of storage and offloading will then eliminate necessity to lay the expensive long distance of using pipeline. The transport of product is done by LNG/Oil shuttle tanker that comes regularly. The other benefit when it is used in the smaller oil field which can be exhausted in few years is that the owner can decide to move the FPSO to other places after the operation finish.

There are three types of mooring system in FPSO; spread mooring, external turret system and internal turret system (Figure 1).The spread mooring system does not allow vessel to weathervane, therefore turret system is needed in the harsh and deeper area.

Spread Mooring	Turret	
	External Turret System	Internal Turret System
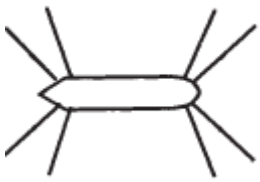		

Figure 1 FPSO Mooring System[3]

Nowadays, other than crude oil natural gas is also used as energy sources. The Liquid Natural Gas is natural gas which through a process of liquefactions. It stored and transport in very low temperature, approximately -160^0 C. Hence many research concern on developing the FPSO used for LNG. Some important considerations are taken due to the characteristic of LNG, for instance offloading process storage system, and sloshing due to motion of the vessel.

There are two methods of offloading process for oil transfer i.e. tandem and side-by-side configuration. For tandem configuration, LNG tanker is moored in tandem with the FPSO. The hoses (or hawsers) are connected between the stern off-loading stations on FPSO to the cross over manifold of the tanker. While, the side-by-side configuration is done by moored the tanker parallel with the FPSO and off-loading is carried out via a flexible hose between the cross over manifold of the FPSO and tanker.

1.2. Development Study of New Concept FPSO in LNG Production

New concept of FPSO with cylinder shape is developed by Sevan Marine[4]. The other advantages of the cylindrical shape are the flexibility design and favorable motion characteristic sustain the FPSO used both in deep and shallow waters. It uses spread mooring system without the turret and swivel as its station-keeping manner. Sevan FPSO has high capacity of deck load with the main component on deck are living quarters with control rooms, workshop, live vessels, helipad, cranes, on- and offloading system for the product, and anchor winches. The hull is designed for the machinery, power generators, transformators, electric boards, fire control system, ballast pump and cargo pumps. Three of the Sevan FPSO are operated in Brazil and North Sea.

And currently, the study of Sevan FPSO in application of LNG production is still being developed. As explained before, due to the low temperature of the LNG then the offloading system is more complicated compare with oil. Here, the flexible hose cannot be used. The offloading process is only allowed to be moved by using a loading-arm. And the consequent are both of the FPSO and LNG Shuttle Tanker need to be close to each other (Figure 2).

Figure 2 Master plan of LNG offloading process (provided by Sevan Marin ASA)

1.3. Contribution of This Report

Study of offloading system and cyclonic conditions for Sevan FPSO has been perform in 2007 by Sevan Marin ASA[5]. The purpose is to establish and verify an offshore offloading solution for Sevan FPSO based on use of standard shuttle tankers. The analysis is applicable for oil offloading system.

In this report, the study is extended in application for LNG offloading system. During the offloading process using loading arm, large dimension of cylindrical FPSO which is located very close to the LNG Shuttle tanker will produce hydrodynamic interaction. In addition, there is also complex mooring system need to be considered.

The emphasis of this report is to establish the LNG offloading configuration and study the influence of hydrodynamic interaction during offloading process. Here is also performed the mooring line analysis to ensure that the mooring system has enough capacity to keep both of cylindrical FPSO and LNG shuttle tanker in certain position during the offloading process. The study covers the following activities below.

1. Study Literature of LNG offloading process, floating structures in regular waves, multi body analysis, irregular waves and nonlinear problem, and mooring system.
2. Study literature of the basic theory of the related software used during the analysis i.e. SESAM (Wadam and Genie) and SIMO.
3. Perform the multi-body and mooring analysis.

And the solutions from this study are aimed to answer the following problems.

1. What's the LNG offloading configuration propose for the analysis?
2. How's the influence from hydrodynamic interaction into multi-body model in regular waves?
3. How's the offloading system performance in varying sea-state?
4. How's the influence from hydrodynamic interaction into the offloading system?
5. How's the effect from wind and current load into the offloading system performance?
6. Does the mooring system meet the requirement for MBL (Minimum Breaking Load)?

In order to solve the problems above, the analysis is mainly divided into 2 parts i.e. frequency domain analysis and time domain analysis. In frequency domain analysis, the software used is WADAM. While, in time domain analysis, the software used is SIMO.

Ideally the optimization of offloading configuration is taken to get the most efficiency in mooring system. However, since the emphasis of this study is the influence of hydrodynamic interaction therefore the analysis is limited in one mooring configuration.

1.4. Outline

As explained in the previous chapter regarding the aim of this study, here will be described the outline of this report. In general, it will be divided in to eight chapters. The explanation of each chapter will be discussed in points below.

1. Chapter 1 Introduction

   In chapter 1, the discussion is about FPSO and its advantages, type of offloading configuration and also discussed the development of new concept of FPSO.

2. Chapter 2 Floating Structures in Regular Waves

   This chapter gives basic knowledge of doing floating structures analysis in regular waves. Started from the basic theory of single body analysis then expand to the application for multi- multi-body analysis.

3. Chapter 3 Non-Linear Problems

   This chapter explains the effect of second order waves in moored structures. Here is also discussed the wind and current forces. And the last part, the discussion of time domain analysis.

4. Chapter 4 Mooring System

   In chapter 4, it explains the type of methods in order to perform mooring analysis. Started from catenary equation, quasi static design, dynamics design and coupling line calculation.

5. Chapter 5 Multi-body Analysis in Regular Waves

   In this chapter present the FPSO and LNG Tanker data, modeling concept in WADAM and calculation the hydrodynamic coefficient of the structures in regular waves.

6. Chapter 6 Hydrodynamic interaction in Offloading System

   In chapter 6, it presents the offloading system configuration, equilibrium analysis and decay test analysis. In the last part, it is discussed the Offloading system performance in varying sea-state and also study of the influence from hydrodynamic interaction in the offloading system.

7. Chapter 7 Mooring Analysis

   This chapter explains the mooring analysis in SIMO. Here is also presented the result of analysis and discussions.

8. Chapter 8 Conclusion and Recommendation

   In this chapter summarize of the all previous step and some recommendation is propose for further work.

CHAPTER II FLOATING STRUCTURES IN REGULAR WAVES

This chapter explains the basic theory of the analysis. Start from the coordinate system, regular sea waves, structures response in regular waves, and frequency domain analysis.

2.1. Rigid Body Dynamics

First of all it is important to understand the body coordinate system of the structures. It is differences between single body and multi-body coordinate system in the analysis. I wil be explained the coordinate system used for the analysis in WADAM and Figure 3 presents clearly description of it.

Motion of the rigid body can be split into three translations about the COG and three rotations around COG. The right handed orthogonal coordinate system is used to define the ship motion[6].

- The global coordinate system (X_{glo}, Y_{glo}, Z_{glo}) with its origin at still water level and with the z-axis normal to the still water level and the positive z-axis pointing upwards.
- The individual body coordinate systems (X_B, Y_B, Z_B) of each structure are specified relative to the global coordinate system.
- The input coordinate system (X_{inp}, Y_{inp}, Z_{inp}) of each input model included in a body is specified relative to the body coordinate system of that body.

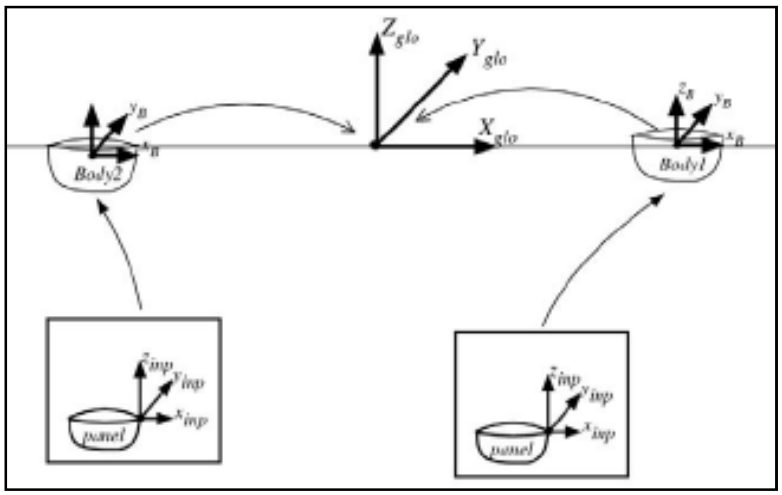

Figure 3 Multi-body Coordinate System in WADAM [6]

Further, the oscillatory rigid body translatory motions can be referred as surge, sway and heave. While, the oscillatory angular motions referred as roll, pitch and yaw (Figure 4).

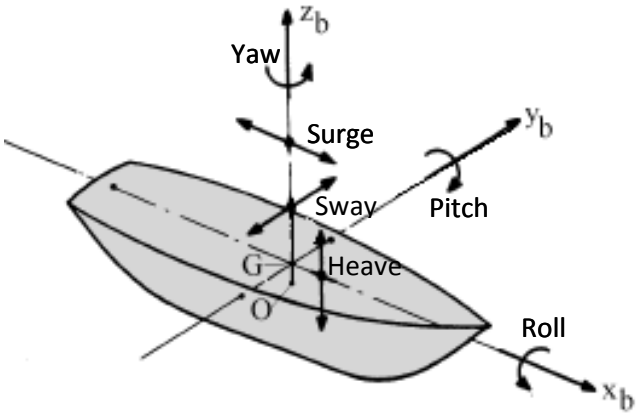

Figure 4 Definition of Ship Motion in Six Degrees of Freedom[7]

In the single body analysis, the result refers to the global coordinate system. While, in multi-body analysis the result refers to the own body coordinate system[7].

2.2. Regular Sea Waves

There is hydrodynamic classification in the analysis which depends on the types of structures[8]. In Figure 5 below describes the classification of hydrodynamic term that dominant on the structures.

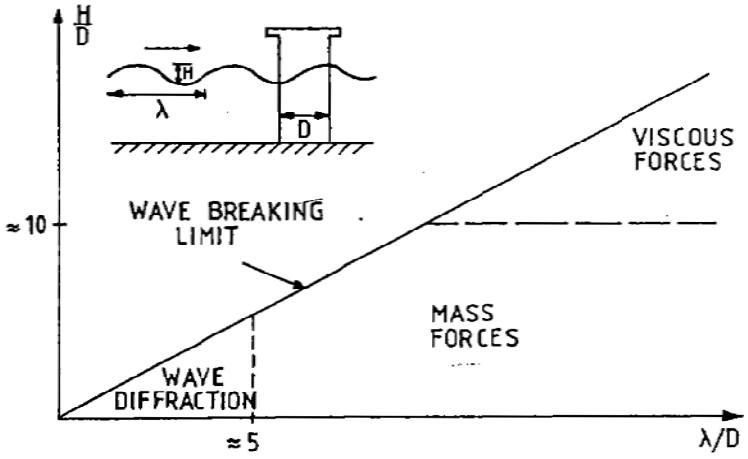

Figure 5 Relative importance of mass, viscous drag and diffraction forces on marine structures[8]

Furthermore, the next discussion in sub-chapter 2.2.1 and 2.2.2 refer to [6, 8].

2.2.1. Potential Theory

Refer to the Figure 5 above; In order to analyze the hydrodynamic loads on floating structures with large volume the potential flow effect is more important than the viscous effect.

Furthermore, when the boundary layer is small, the amount of fluid is effectively *ideal*. By assuming the ideal fluid, i.e. inviscid and incompressible, then the motion of the fluid is to be irrotational. In that's condition, the velocity vector **V** can be represented by the gradient of a scalar potential ϕ which depends generally on three x_i and time t.

Equation 1

$$\mathbf{V} = \boldsymbol{\nabla}\phi \equiv \frac{\partial\phi}{\partial \mathrm{x}}\,\mathbf{i} + \frac{\partial\phi}{\partial \mathrm{y}}\mathbf{j} + \frac{\partial\phi}{\partial \mathrm{z}}\,\mathbf{k}$$

Where, **i, j,** and **k** are unit vector along the x-, y- and z-axes respectively. Recall the condition that the water is incompressible,

Equation 2

$$\boldsymbol{\nabla}.\mathbf{V} = \mathbf{0}$$

Thus,

Equation 3

$$\frac{\partial^2\phi}{\partial \mathrm{x}^2} + \frac{\partial^2\phi}{\partial \mathrm{y}^2} + \frac{\partial^2\phi}{\partial \mathrm{z}^2} = 0$$

This is the *Laplace equation* which expresses conservation of fluid mass for potential flows and provides the governing partial differential equation to be solved for the function ϕ.

Furthermore, the pressure p follows from Bernoulli's equation. If we assume that z-axis to be vertical positive upwards we express as

Equation 4

$$p + \rho g z + \rho\frac{\partial\phi}{\partial \mathrm{t}} + \frac{\rho}{2}\mathbf{V}.\mathbf{V} = \mathrm{C}$$

Where, C is an arbitrary function of time. And then, includes the time dependence of C in the velocity potential and keep C be a constant.

2.2.2. Boundary Conditions

The distinction between different types of fluid motion resulted from the condition of the boundaries imposed on the fluid domain. Two types of boundary condition are:

- Kinematic boundary conditions

  It is corresponding with the velocity of the fluid on the boundary. The kinematic body boundary condition of the rigid body with translatory and rotary motion is expressed as below

Equation 5

$$\frac{\partial \phi}{\partial \mathrm{n}} = \mathbf{U}.\mathrm{n} \quad \text{on body surface}$$

Where, $\mathbf{U}$ is body velocity and n is unit vector which is defined to point normal out from the body. For fix body the equation above become

Equation 6

$$\frac{\partial \phi}{\partial \mathrm{n}} = 0 \quad \text{on body surface}$$

The equation above means that no fluid trough to the body.

While, the kinematic free surface is defined as $z = \zeta(x, y, t)$. Where, ζ is the wave elevation. Then, we define the function

Equation 7

$$\mathrm{F}(\mathrm{x}, \mathrm{y}, \mathrm{z}, \mathrm{t}) = \mathrm{z} - \zeta(x, y, t) = 0$$

A fluid particle on the free surface is assumed to stay on the free-surface. It is means that the expression below

Equation 8

$$\frac{\mathrm{DF}}{\mathrm{Dt}} = \frac{\partial \mathrm{F}}{\partial \mathrm{t}} + \mathbf{V}.\boldsymbol{\nabla}\mathrm{F} = 0$$

$$\frac{\partial}{\partial \mathrm{t}}\big(\mathrm{z} - \zeta(x, y, t)\big) + \boldsymbol{\nabla}\phi.\boldsymbol{\nabla}\big(\mathrm{z} - \zeta(x, y, t)\big) = 0$$

$$\frac{\partial \zeta}{\partial \mathrm{t}} + \frac{\partial \phi}{\partial \mathrm{x}}\frac{\partial \zeta}{\partial \mathrm{x}} + \frac{\partial \phi}{\partial \mathrm{y}}\frac{\partial \zeta}{\partial \mathrm{y}} - \frac{\partial \phi}{\partial \mathrm{z}} = 0 \quad \text{on } \mathrm{z} = \zeta(x, y, t)$$

And, the kinematic sea floor boundary condition is expressed as

Equation 9

$$\frac{\partial \phi}{\partial \mathrm{n}} = 0 \quad \text{on sea floor}$$

- Dynamic boundary conditions

  It is corresponding with the forces on the boundary. In free-surface, the boundary condition is simply that the water pressure is equal to the constant atmospheric pressure p_0 on the free-surface. If we choose the constant coefficient C in Equation 4 equal to the $\frac{p_0}{\rho}$ so that the equation holds with no fluid motion, then the formula become:

Equation 10

$$g\zeta + \frac{\partial \phi}{\partial t} + \frac{1}{2}\left(\left(\frac{\partial \phi}{\partial x}\right)^2 + \left(\frac{\partial \phi}{\partial y}\right)^2 + \left(\frac{\partial \phi}{\partial z}\right)^2\right) = 0 \text{ on } z = \zeta(x, y, t)$$

But, here we do not know where the free-surface is before the problem solved. By linearizing the free-surface condition the problem is be able to solve. We assume that the structure has no speed and the current is zero. The linear theory means that the velocity potential is proportional relation with the wave amplitude. The equation become

Equation 11

$$g\zeta + \frac{\partial \phi}{\partial t} = 0 \quad \text{on } z = 0$$

From the kinematic free surface boundary condition, we get

Equation 12

$$\frac{\partial \zeta}{\partial t} = \frac{\partial \phi}{\partial z} = 0 \quad \text{on } z = 0$$

2.2.3. Regular Waves Theory

In first order potential theory, waves are modeled as Airy wave theory. The derivation of the formula can be found in [9] and [10]. The velocity potential expressed as below.

Equation 13

$$\phi = \frac{gA}{\omega}\frac{\cosh k(z + d)}{\cosh kd}\sin(kx - \omega t)$$

The incident waves are represented as the wave length, wave angular frequencies or wave periods. The direction of the incident waves are specified by β between the positive x-axis and the propagation directions [7].

In complex form the incident wave is expressed as:

Equation 14

$$\zeta = Re\left[Ae^{i(\omega t - k(x\cos\beta + y\sin\beta))}\right]$$

Equation 15

$$\zeta = Acos\ (\omega t - k(x\cos\beta + y\sin\beta))$$

The wave propagation direction and wave phase is represented as figure below.

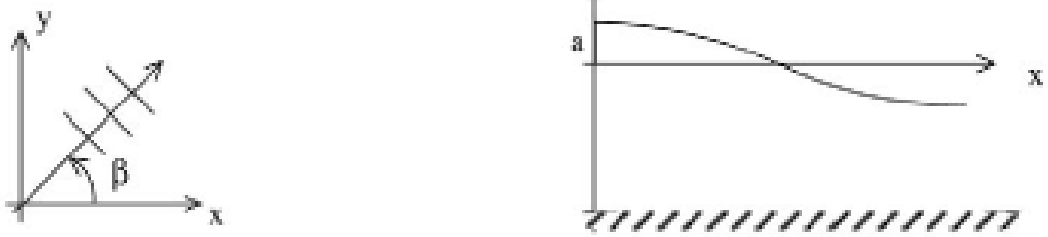

a. Wave propagation direction

b. wave phase at t = 0

Figure 6 Surface waves definition[7]

The fluid velocity $v = v_x\boldsymbol{i} + v_y\boldsymbol{j} + v_z\boldsymbol{k}$ and $a = a_x\boldsymbol{i} + a_y\boldsymbol{j} + a_z\boldsymbol{k}$ for the incident waves are:

Equation 16

$$v_h = v_x\boldsymbol{i} + v_y\boldsymbol{j} = A\omega\frac{\boldsymbol{k}}{k}\frac{\cosh(kz+kd)}{\sinh(kd)}\cos(\omega t - \boldsymbol{k}.\boldsymbol{x})$$

Equation 17

$$v_z = -A\omega\frac{\sinh(kz-kd)}{\sinh(kd)}\sin(\omega t - \boldsymbol{k}.\boldsymbol{x})$$

Equation 18

$$a_h = -a_x\boldsymbol{i} + a_y\boldsymbol{j} = A\omega^2\frac{\boldsymbol{k}}{k}\frac{\cosh(kz+kd)}{\sinh(kd)}\sin(\omega t - \boldsymbol{k}.\boldsymbol{x})$$

Equation 19

$$a_z = -A\omega^2\frac{\boldsymbol{k}}{k}\frac{\sinh(kz+kd)}{\sinh(kd)}\cos(\omega t - \boldsymbol{k}.\boldsymbol{x})$$

Where, the still water level is obtained by constant extrapolation in WADAM.

2.3. Structure Response in Regular waves

The basic theory related with analyzing single body response is explained clearly in [6] and [8]. While, the understanding of multi-body response analysis gained from journals [11-21].

2.3.1. Single Body

Consider the structure in incident regular wave with linear theory applied, i.e. the wave induced motion and load amplitudes are linearly proportional to ζ_a. The advantages of using linear theory is that we can determine the response in irregular sea by adding together the result from regular waves of different amplitudes, wave lengths and propagation directions[8].

For floating structure, the hydrodynamics problem can be separated into main two sub-problems[6, 8].

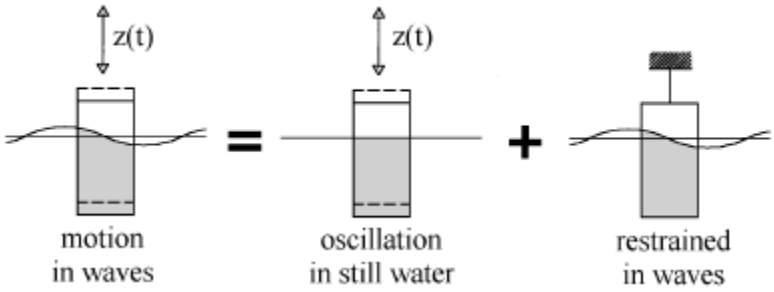

Figure 7 Superposition in Hydro mechanical and Wave Loads[6]

The first sub problem, forces and moment on the body when the structures is oscillated, there are no incident waves. The oscillation itself causes the fluid oscillation on the body surface and the integration over the body surface will give us the result of the forces and moments on the body.

By given $\Phi(\vec{r},t)$ the fluid pressure, p is calculated as follow:

Equation 20

$$p = -\rho \frac{\Phi(\vec{r},t)}{dt}$$

And then, Force in each body element can be expressed as

Equation 21

$$d\vec{F} = p.(-\vec{n}).dA$$

The total force, $\vec{F}$ on the body is obtained by integrate the formula above along the body surfaces. Here, the added mass and damping term due to the harmonic motion also be able to

determine. The restoring forces and moment is calculated depend on the hydrostatic and mass consideration. In special case, e.g. moored structures the additional restoring forces from the mooring stiffness have to be taken in to account.

Second sub problem, forces and moment on the body when the structure is restrain from the oscillatory and there are incident waves. The corresponding forces and moment is called Froude-Kriloff and Diffraction forces and moment. The Froude-Kriloff force is produces from the undisturbed pressure field, while the diffraction force is come from the changes of pressure field on the structure.

Diffraction forces can be solved as similar way as added mass and damping calculation but the difference is the boundary condition in the body, where the normal derivative of the diffraction velocity potential has to be opposite and of identical magnitude as the normal velocity of the undisturbed wave system. The total of hydrodynamic forces and moments are obtained from the summation of those two sub-problems [8].

Below is the concept of how WADAM calculate the potential velocity [7]. Start from follows the Laplace equation, the velocity potential is given by:

Equation 22

$$\nabla^2 \Phi = 0$$

The harmonic time dependence accept for defining a complex velocity potential ϕ related to Φ by

Equation 23

$$\Phi = \mathrm{Re}\,(\phi\, e^{i\omega t})$$

Where ω frequency of incident wave and t is is time. The linearized form for free surface condition is expressed as

Equation 24

$$\phi_z - K\phi = 0 \qquad z = 0$$

k is wave number $(\frac{\omega^2}{g})$ and g is acceleration of gravity. Further, the potential of incident wave is determined by

Equation 25

$$\phi_0 = \frac{igA}{\omega}\frac{\cosh(kz+H)}{\cosh kH} e^{-k(x\cos\beta + y\sin\beta)}$$

As written above that the wave number k is the real root of the dispersion relation and β is the angle between the direction of propagation of the incident wave and the positive x-axis. Linearization the problem that the total velocity on single body is written as:

Equation 26

$$\phi = \phi_R + \phi_D$$

Radiation potential, ϕ_R is written as below, where ξ_j is the complex amplitudes of the body oscillatory motion in its six degree of freedom and ϕ_j is the corresponding unit amplitude radiation potentials.

Equation 27

$$\phi_R = i\omega \sum_{j=1,6} \xi_j \phi_j$$

The diffraction potential, ϕ_D is expressed as the summation of velocity comes from the disturbance of the incidence wave by the body fixed at its undisturbed position and the incident wave potential.

Equation 28

$$\phi_D = \phi_0 + \phi_7$$

2.3.2. Multi Body

For multi-bodies problem, the interaction between the structures has to be considered. The basic theory below is refer to [18]. The diffraction potential for the isolated body can be defined by the incident potential as expressed as below.

Equation 29

$$\frac{\partial \phi_7^I}{\partial n} = -\frac{\partial \phi_0}{\partial n} \qquad \text{on} \quad S_I$$

Equation 30

$$\frac{\partial \phi_7^{II}}{\partial n} = -\frac{\partial \phi_0}{\partial n} \qquad \text{on} \quad S_{II}$$

Where S_I and S_{II} denotes the wetted surface of the isolated body I and II respectively. ϕ_7^I and ϕ_7^{II} denotes the scattered potential to the isolated body I and II. ϕ_0 is the incident wave potential of the isolated body. The radiation potential for the isolated body can be decomposed in the similar way to the single body.

Equation 31

$$\phi_R^I = i\omega \sum_{j=1,6} \xi_j \phi_j^I$$

Equation 32

$$\phi_R^{II} = i\omega \sum_{j=1,6} \xi_j \phi_j^{II}$$

The radiation problem for the isolated body I and II can be given as follow

Equation 33

$$\frac{\partial \phi_j^I}{\partial n} = n_j^I \qquad \text{on} \quad S_I \quad (j = 1,2,\dots,6)$$

Equation 34

$$\frac{\partial \phi_j^{II}}{\partial n} = n_j^{II} \qquad \text{on} \quad S_{II} \quad (j = 1,2,\dots,6)$$

Where ϕ_j^I and ϕ_j^{II} denotes the decomposed radiation potential components for the isolated body I and II respectively and $n_j^{I,II}$ is a unit normal normal vector for the six degree of freedom for the isolated body I and II. The formulas are given below:

Equation 35

$$n_j^{I,II} = \begin{cases} (n_1, n_2, n_3)^{I,II} & \text{for } j = 1,2,3 \\ (n_4, n_5, n_6)^{I,II} = \breve{r} \times n & \text{for } j = 1,2,3 \end{cases}$$

Where $\breve{r}$ denotes the relative distance from the origin to each other body center.

The boundary-value equation and the boundary condition for each body of the interaction problem are defined in the form of the radiation/scatter potential. The derivation of the formula is written as follows:

- Condition 1: Radiation from I near II (Body I is oscillating and body II fixed)

Equation 36

$$\frac{\partial \hat{\phi}_j^I}{\partial n} = -\frac{\partial \phi_j^I}{\partial n} \qquad \text{on} \quad S_I \quad (j = 1,2,\dots,7)$$

Equation 37

$$\frac{\partial \hat{\phi}_j^I}{\partial n} = 0 \qquad \text{on} \quad S_{II} \quad (j = 1,2,\dots,7)$$

- Condition 2: Radiation from II near I (Body II is oscillating and body I fixed)

Equation 38

$$\frac{\partial \hat{\phi}_j^{II}}{\partial n} = -\frac{\partial \phi_j^{II}}{\partial n} \qquad \text{on} \quad S_{II} \quad (j = 1,2,\dots,7)$$

Equation 39

$$\frac{\partial \hat{\phi}_j^{II}}{\partial n} = 0 \qquad \text{on} \quad S_I \quad (j = 1,2,\dots,7)$$

Where $\hat{\phi}_j^I$ denotes the interaction potential affected by radiation/ scatter potential from the body I to the body II and $\hat{\phi}_j^{II}$ is the potential affected by radiation/scatter potential from the body II to the body I. The potential when j = 7 means the scatter term.

Then, the hydrodynamics coefficient is solved in to two sequences as follows:

1. The radiation/diffraction problem for each body in isolation
2. The interaction problem resulting from radiation of body I influence to the body II, and vice versa.

Where body I and II represent one pair of bodies which interact hydro dynamically. Thereafter the boundary value problem is solved by using Equation 38 – Equation 39 in terms of excitation force coefficient as follows.

Equation 40

$$C_j^{I,I} = -\int_{S_I} a\hat{\phi}_7^I \, n_j \, dS, \qquad (j = 1,2,\dots,6)$$

Equation 41

$$C_j^{II,II} = -\int_{S_I} a\hat{\phi}_7^{II} \, n_j \, dS, \qquad (j = 1,2,\dots,6)$$

Equation 42

$$C_j^{I,II} = -\int_{S_I} a(\hat{\phi}_7^{II} + \phi_7^{II}) n_j \, dS, \qquad (j = 1,2,\dots,6)$$

Equation 43

$$C_j^{II,I} = -\int_{S_{II}} a(\hat{\phi}_7^{I} + \phi_7^{I}) n_j \, dS, \qquad (j = 1,2,\dots,6)$$

Below, the hydrodynamic coefficient is expressed in terms of equivalent added mass,

Equation 44

$$M^{a\,I,I}(\infty) = -\int_{S_I} \hat{\phi}_j^I \, n_i \, dS, \qquad (i,j = 1,2,\dots,6)$$

Equation 45

$$M^{a\,II,II}(\infty) = -\int_{S_{II}} \hat{\phi}_j^{II} \, n_i \, dS, \qquad (i,j = 1,2,\dots,6)$$

Equation 46

$$M^{a\,I,II}(\infty) = -\int_{S_I} a(\hat{\phi}_j^{II} + \phi_j^{II}) n_i \, dS, \qquad (i,j = 1,2,\dots,6)$$

Equation 47

$$M^{a\ II,I}(\infty) = -\int_{S_I} a(\hat{\phi}_j^{II} + \phi_j^I) n_i \ dS\,, \qquad (i,j = 1,2,\dots,6)$$

2.4. Frequency Domain Analysis

Since the hydrodynamic coefficient and the exciting wave have been found from the description above, the equation of motion for single body can be expressed as

Equation 48

$$\sum_{k=1}^{6}[(M+A)\ddot{\eta} + B\dot{\eta} + C\eta] = Fe^{-iw_e t}$$

Where *M, A, B and C* is the generalized mass, added mass, damping and restoring matrix for the structures respectively. *F* is the complex amplitudes of exiting forces and moment component given by the real part of $Fe^{-iw_e t}$.

By expanding the equation of motion for single body, the expression for multi bodies problems can be expressed as below [15, 18, 22].

Equation 49

$$\sum_{k=1}^{6}[(M^1 + A^{11} + \dots + A^{1N})\ddot{\eta} + (B^{11} + \dots + B^{1N})\dot{\eta} + C^1\eta] = F^1 e^{-iw_e t}$$

$$\vdots \qquad\qquad \vdots$$

$$\sum_{k=1}^{6}[(M^N + A^{N1} + \dots + A^{NN})\ddot{\eta} + (B^{N1} + \dots + B^{NN})\dot{\eta} + C^N\eta] = F^N e^{-iw_e t}$$

Superscript denotes the mode number of interaction between N bodies.

When the body is oscillated by harmonic waves, the corresponding response will be harmonic functions. The transfer function, H(ω,β) gives the ratio between response amplitude and incident wave amplitudes. The corresponding time dependent response variable R(ω,β,t) can be expressed as

Equation 50

$$R(\omega, \beta, t) = ARe\left[H((\omega, \beta))e^{i\omega t}\right]$$

Where A is the amplitude of incoming wave, ω is the frequency of incoming wave, β describes the direction of the incoming wave and t denotes time.

The phase angle **ϕ** between the incident wave and the time varying response is defined from

Equation 51

$$R(\omega, \beta, t) = ARe\left[|H(\omega, \beta)|e^{i\omega t + \phi}\right]$$

|H| is the amplitude of the transfer function. The transfer function and the phase angle can be expressed as

Equation 52

$$H = H_{Re} + H_{Im}$$

And

Equation 53

$$\phi = \text{atan}\frac{H_{Im}}{H_{Re}}$$

The time varying response can alternatively be expressed as

Equation 54

$$R(\omega, \beta, t) = A[H_{Re}cos\omega t - H_{Im}sin\omega t]$$

CHAPTER III NON LINEAR PROBLEMS

In previous chapter the response calculation is developed from linearized Bernaulli's equation. Further, In order to solve the problem as close as the real condition so we need to consider the higher order term. Following will be discussed the second order wave forces, wind and current forces and the time domain analysis.

3.1. Second Order Wave Forces

The effect of the second order wave force is most apparent in the behavior of the moored structures. In regular wave, the simple way to present the non-linear effect in wave is by consider the complete Bernaulli's equation[8].

Equation 55

$$\frac{1}{2}\rho|\nabla\phi|^2 = \frac{1}{2}\rho(u^2 + v^2 + w^2)$$

Where $\nabla\phi$ = (u, v, w) is fluid velocity vector. In idealilized sea state, an approximation of x-component velocity which consist of circular frequency ω_1 and ω_2 can be written as

Equation 56

$$u = \mathrm{A}_1\cos(\omega_1 t + \epsilon_1) + \mathrm{A}_2\cos(\omega_2 t + \epsilon_2)$$

$$v = 0$$

$$w = 0$$

By introducing Equation 56 to Equation 55 we get result as follow.

Equation 57

$$\frac{1}{2}\rho|\nabla\phi|^2 = \frac{1}{2}\rho\frac{{\mathrm{A}_1}^2}{2} + \frac{1}{2}\rho\frac{{\mathrm{A}_2}^2}{2}$$

$$+\frac{1}{2}\rho\frac{{\mathrm{A}_1}^2}{2}cos(2\omega_1 t + \epsilon_1)$$

$$+\frac{1}{2}\rho\frac{{A_2}^2}{2}cos(2\omega_2 t+\epsilon_2)$$

$$+\frac{1}{2}\rho A_1 A_2 cos((\omega_1-\omega_2)t+(\epsilon_1-\epsilon_2))$$

$$+\frac{1}{2}\rho A_1 A_2 cos((\omega_1+\omega_2)t+(\epsilon_1+\epsilon_2))$$

As shown in the formula above, the result is divided into three component; mean wave (drift) forces, forces oscillating in difference frequencies and forces oscillating in sum frequencies. Mean forces and forces oscillating in difference frequencies are more importance in moored structures. Study regarding mean forces and slow drift also has been done by[23-25].

3.1.1. Mean Wave (Drift) Forces

In order to calculate mean wave load in structures, it is not necessary to solve the second-order potential because the time dependence over the one period oscillation of the pressure is zero. It means that the second order potential does not result in mean loads. Two methods of calculating mean (wave) drift forces are conservation of momentum and direct pressure method[8]. The conservation momentum method is more efficient and less demanding numerical discretisation, while direct pressure method is more useful if the solution will be extended to calculate time harmonic second order forces[26].

In conservation of momentum method, the volume integral is reduce to the surface integral by using vector algebra and a generalized Gauss theorem[8]. Hereafter, the expression of momentum conservation can be written as follow.

Equation 58

$$\frac{\partial \boldsymbol{M}}{\partial t}=-\rho\iint_S\left[\left(\frac{p}{\rho}+gz\right)\boldsymbol{n}+\boldsymbol{V}(V_n-U_n)\right]ds$$

Where $V_n=\frac{\partial\Phi}{\partial n}$ is the normal component of the fluid velocity at the surface.

Maruo(1960) derived mean drift forces equation by applied the boundary condition in the body surface S_B, sea floor S_0, non-moving circular cylinder surface S_∞, and the free surface S_F.

Equation 59

$$\overline{F_i} = -\iint_{S_\infty} [pn_i + \rho V_i V_n] ds \qquad i = 1,2$$

Based on the equation above, Maruo(1960) also derived the formula for drift force, $\overline{F_i}$ on two-dimensional body in incident regular deep water. The basic idea is that the structure ability to create waves. By integrated the pressure over the wetted surface which is correctly into second-order wave amplitude and solved the boundary condition then the result was written as

Equation 60

$$\overline{F_2} = -\frac{\rho g}{2} {A_R}^2$$

Where A_R is a reflected waves. In condition that wave length is very large compare to the body, there will be very small reflected wave, i.e that A_R is close to zero. While, in the short wave length A_R is equal to ζ_a. In large motion of the body the mean drift may have peak in the frequency range of resonance[8]. The similar formula has been derived by Newman (1967) for mean wave-drift in yaw moment. By using the fluid angular momentum he concluded that the Equation 59 is also valid for yaw moment.

Direct integration method was derived by Pinkster & van Oortmerssen (1977) by using complete bernaulli's equation for the pressure and integrates over the hull to second order wave amplitude. Here, all three force component and three moment can be found. By analyzed the incident regular deep water waves on vertical wall, the asymptotic value agreed with the Maruo's formula.

Equation 61

$$\overline{F_i} = \int_{-\infty}^{\zeta} \left(-\rho g z - \frac{\partial \phi_1}{\partial t} - \frac{\rho}{2} \left(\left(\frac{\partial \phi_1}{\partial y} \right)^2 + \left(\frac{\partial \phi_2}{\partial z} \right)^2 \right) \right) dz$$

$$= \rho g {\zeta_a}^2 - \frac{1}{2} \rho g {\zeta_a}^2 = \frac{1}{2} \rho g {\zeta_a}^2$$

The generalized asymptotic formula for vertical wall can be written as

Equation 62

$$\overline{F_i} = \frac{1}{2}\rho g {\zeta_a}^2 \int_{L_1} \sin^2(\theta + \beta) n_i dl$$

Where θ is the wave propagation direction. And β is the angle between tangential surface and horizontal line.

Further, the mean drift in irregular sea can be found from the result in regular sea by assuming the long-crested sea described by sea spectrum. The formula is written as follow.

Equation 63

$$\overline{F_i^S} = 2\int_0^\infty S(\omega)\left(\frac{\overline{F_i}\,(\omega;\beta)}{{\zeta_a}^2}\right)d\omega \qquad i = 1,\dots,6$$

3.1.2. Slowly Varying Wave Forces

Slow drift motion are resonance oscillations excited by non-linear interaction effects between the waves and the body motion[8]. It is important for moored structure the resonance oscillation occurs in surge, sway and yaw. Slow drift excitation load can be determined by similar formula with mean drift in irregular sea but the second order potential needs to be included. Based on the Equation 57 line 4 the slowly-varying force, F_i^{SV} can be determine by introduce N wave components and include all second-order contribution. The formula is expressed as

Equation 64

$$F_i^{SV} = \sum_{j=1}^{N}\sum_{k=1}^{N} A_j A_k \left[T_{jk}^{ic} cos\{(\omega_k - \omega_j)t + (\epsilon_k - \epsilon_j)\} + T_{jk}^{is} sin\{(\omega_k - \omega_j)t + (\epsilon_k - \epsilon_j)\}\right]$$

Where T_{jk}^{ic} and T_{jk}^{is} are second-order transfer function for the difference frequency loads. Bu using Newman (1974) definition as below, the Equation 64 can be solved efficiently.

Equation 65

$$T_{jk}^{ic} = T_{kj}^{ic} \text{ And } T_{jk}^{is} = T_{kj}^{is}$$

Further, the mean value of Equation 64 can be found by

Equation 66

$$\overline{F_i^{SV}} = \sum_{j=1}^{N} \mathrm{A_j}^2 \, T_{jj}^{ic}$$

The basic idea from Newman Approximation is that T_{jk}^{ic} and T_{jk}^{is} can be expressed in term of T_{jj}^{ic}, T_{kk}^{ic}, T_{jj}^{is} and T_{kk}^{is}.

Equation 67

$$T_{jk}^{ic} = T_{kj}^{ic} = 0.5\,(T_{jj}^{ic} + T_{kk}^{ic})$$

$$T_{jk}^{is} = T_{kj}^{is} = 0$$

The other approximation from Newman is by approximate the double summation by the square of a single series.

Equation 68

$$F_i^{SV} = 2\left(\sum_{k=1}^{N} \mathrm{A_j}(T_{jj}^{ic})^{\frac{1}{2}} \cos\,(\omega_j t + \epsilon_j)^2\right)$$

According to Pinkster (1975), the spectral density of the low frequency part can be found by

Equation 69

$$S_F(\mu) = 8\int_0^{\infty} S(\omega)S(\omega+\mu)\left(\frac{\overline{F_i}\left(\omega+\frac{\mu}{2}\right)}{{\zeta_a}^2}\right)^2 d\omega$$

Where $\overline{F_i}\left(\omega+\frac{\mu}{2}\right)$ is the mean wave load in direction i for frequency $\omega+\frac{\mu}{2}$.

3.2. Wind and Current Forces

Wind and current force is also important in design moored structures[27]. The fluctuating force might be lead to resonance oscillations of offshore structures.

3.2.1. Current Loads on Ship

Surface current on the ship is coming from local wind, tidal component, stokes drift, ocean circulation, local density-driven current and set-up phenomena[8]. The total current is the vector sum of these currents, and the speed and direction of the current at specified water depths are represented by a current profile[28]. The surface current may affect drift in ship or floating structures.

Current loads on the ship can be representing by drag force in longitudinal direction due to the frictional forces. The calculation procedure follows the ship resistance estimation. Here, the viscous resistance is more dominant than wave resistance[8]. The estimation formula is written as follow.

Equation 70

$$F_1^c = \frac{0.075}{(\log_{10} Rn - 2)^2}\frac{1}{2}\rho S {U_c}^2 cos\beta|cos\beta|$$

Where β is the angle between current velocity and the longitudinal x-axes. S is the wetted surface of the ship. And Rn is calculated from

Equation 71

$$Rn = \frac{U_c L|cos\beta|}{\upsilon}$$

The other formula to express current force is from Hughes (1954) where $\frac{0.075}{(\log_{10} Rn-2)^2}$ is replaced by $\frac{0.066(1+k)}{(\log_{10} Rn-2.03)^2}$ where k is factor from the experiment. While, the transverse viscous current forces and yaw moment follow the cross flow principle as long as the current direction is not close to the longitudinal axis of the ship. The formula is expressed as below.

Equation 72

$$F_2^c = \frac{1}{2}\rho\left[\int_L dx C_D(x) D(x)\right] {U_c}^2 sin\beta|sin\beta|$$

Equation 73

$$F_2^C = \frac{1}{2}\rho\left[\int_L dx C_D(x)D(x)\right]U_c{}^2 sin\beta|sin\beta| + \frac{1}{2}U_c{}^2(A_{22} - A_{11})sin2\beta$$

Where L is the length of the ship and A_{11}, A_{22} are added mass in surge and sway respectively. The second term of equation(73) is the Munk moment where it can be found by strip theory approach[8].

3.2.2. Wind Loads on Ship

Wind effect on floating structure is divided in two terms, one from the mean speed and the other is from the fluctuation about this mean value. The mean speed is solved similarly as current force, as steady loads. While the fluctuating wind (gust) is described by the wind spectrum[28].

The NPD wind spectrum is used for strong wind conditions the design wind speed, $u(z,t)$(m/s) at height z (m) above sea level and corresponding to an averaging time period $t \leq t_0 = 3600s$ is given by[29]:

Equation 74

$$u(z,t) = U(z)\left[1 - 0.4\, I_u(z) ln\left(\frac{t}{t_0}\right)\right]$$

Where the 1 hour mean wind speed $U(z)$ (m/s) is given by

Equation 75

$$U(z) = U_0\left[1 + C\, ln\left(\frac{z}{10}\right)\right]$$

Equation 76

$$C = 5.73\, 10^{-2}(1 + 0.15\, U_0)^{\frac{1}{2}}$$

And the turbulent intensity factor $I_u(z)$ is given by

Equation 77

$$I_u(z) = 0.06[1 + 0.043U_0]\left(\frac{z}{10}\right)^{-0.22}$$

Note that U_0 (m/s) is the 1 hour mean wind speed at 10m. For structure which the wind fluctuations are important, the wind spectrum for longitudinal wind speed fluctuations shall use the formula below.

Equation 78

$$S(f) = \frac{320\left(\frac{U_0}{10}\right)^2\left(\frac{z}{10}\right)^{0.45}}{(1+f_m^n)^{\frac{5}{3n}}}$$

And

Equation 79

$$f_m = 172\, f\left(\frac{z}{10}\right)^{\frac{2}{3}}\left(\frac{U_0}{10}\right)^{-0.75}$$

Where n=0.468 and $S(f)$ is the spectral density at frequency f(Hz).

Wind gust with significant energy can also produce slowly varying oscillation in marine structures with high natural periods[8]. With assumption that the structure is sufficiently small, the horizontal force on the body in wind direction can be written as

Equation 80

$$F_D = \frac{1}{2}\rho_{air} C_D A U^2(t)$$

Equation 81

$$U(t) = \bar{U} + u'$$

Where $\bar{U}$ is the mean wind velocity and u' is the fluctuating winds velocity. And the mass density of air is 1.21 kg m^{-3} at 20^0 C. Further, the mean drag force is expressed as

Equation 82

$$F_D = \frac{1}{2}\rho_{air} C_D A \bar{U}^2$$

And the fluctuating drag force and gust velocity spectrum can be written as follow

Equation 83

$$F_{D'}(t) = C_D A \rho_{air} \bar{U} u'(t)$$

Equation 84

$$S_F(f) = (C_D A \rho_{air})^2 S(f)$$

The calculation of slowly varying wind is the same as the calculation on slowly varying wave. For example, if we consider the mean square of surge motion is

Equation 85

$$\sigma_x{}^2 = S_F{}^W(\omega_n)\frac{\pi}{2cb}$$

Where

Equation 86

$$S_F{}^W(\omega)d\omega = S(f)df, \;\; \omega = 2\pi f$$

And the subscribe W means wind.

3.3. Time Domain Analysis

When the system is linear and the incident load only contain first order term then the relation of the load and response will also be linear. And then, the equation of motion is able to solve using frequency domain analysis (see 2.4). However, if there is nonlinear term for instance due to second order wave loads, nonlinear viscous damping, force and moment due to wind and current then the frequency domain approach is not longer valid. To include the nonlinearities as discussed above the equation of motion which follow Newton's second law is solved as a function of time.

The following text is based on [29]. Here, two methods are briefly explained to solve the equation of motion in time domain. If the non-linear terms are included in equation of motion, the expression can be written as follow.

Equation 87

$$[m + A(\omega)]\ddot{x} + C(\omega)\dot{x} + D_1\dot{x} + D_2 f(\dot{x}) + Kx = q_{WI} + q_{WA}^1 + q_{WA}^2 + q_{CU} + q_{ext}$$

Where:

q_{WI} = wind drag force

q_{WI}^1 = 1st order wave excitation force

q_{WI}^2 = 2nd order wave excitation force

q_{CU} = current forces

q_{ext} = any other forces

3.3.1. Solution by Convolution Integral

Here, we directly discuss of convolution integral in application for solving the equation of motion. The detail description of the convolution is clearly explain in [30]. In this method, Equation 87 is separated in terms of frequency dependent component. Where,

Equation 88

$$A(\omega) = A_\infty + a(\omega)\ ;\ A_\infty = A(\omega = \infty)$$

Equation 89

$$C(\omega) = C_\infty + c(\omega)\ ;\ C_\infty = C(\omega = \infty) = 0$$

So we get expression as follow.

Equation 90

$$A(\omega)\ddot{x} + C(\omega)\dot{x} = q_{WI}^1 + q_{WI}^2 + q_{CU} + q_{ext} - M\ddot{x} - D_1\dot{x} - D_2 f(\dot{x}) + Kx$$

The right hand part is sinusoidal oscillating in one single frequency. For harmonic loads, the solution is:

Equation 91

$$-\omega^2 A_\infty X(\omega) + [i\omega a(\omega) + c(\omega)]i\omega X(\omega) = q_{WI}^1 + q_{WI}^2 + q_{CU} + q_{ext} - M\ddot{x} - D_1\dot{x} - D_2 f(\dot{x}) + Kx$$

Further, by using Inverse Fourier Transform the equation above is written as.

Equation 92

$$A_\infty \ddot{x}(t) + \int_0^t h(t-\tau)\,\dot{x}(\tau)d\tau = q_{WI}^1 + q_{WI}^2 + q_{CU} + q_{ext} - M\ddot{x} - D_1\dot{x} - D_2 f(\dot{x}) + Kx$$

Substituting Equation 92 to Equation 90 we get:

Equation 93

$$(M + A_\infty)\ddot{x} + D_1\dot{x} + D_2 f(\dot{x}) + Kx + \int_0^t h(t-\tau)\,\dot{x}(\tau)d\tau = q_{WI}^1 + q_{WI}^2 + q_{CU} + q_{ext}$$

$h(\tau)$ is retardation function which is determined by transform the frequency dependent added mass and damping :

Equation 94

$$h(\tau) = \frac{1}{2\pi}\int_{-\infty}^{\infty}[c(\omega) + i\omega a(\omega)]e^{i\omega t}d\omega$$

For multi body analysis, the coupling retardation also can be determined.

3.3.2. Separation of Motion

In this method, the equation of motion is solved by separates the motion into high frequency and low frequency. Further, the high frequency motion is solve by using the frequency domain and the low frequency motion is solve in time domain. The total motion is summation from both high frequency and low frequency motion.

CHAPTER IV MOORING SYSTEM

In offloading process, mooring system is one of the critical parts. Mooring configuration must be able to provide the restoring force to counteract the structure displacement from the desired position[31]. Mooring lines which made from chain, wire or synthetic rope is attached on the structure and the other end is anchored at the seabed. The pretension of the mooring lines is established by the winch system[8]. Further, the mooring force will be inputted on the equation of motion in time domain[6].

The loading mechanisms acting on the moored floating structure is described in Figure 8. It shows that te load action in the mooring system comes from waves, wind, current load and also from the motion of the vessel[28]. In the next sub-chapter, the type of methods used in mooring analysis will be discussed.

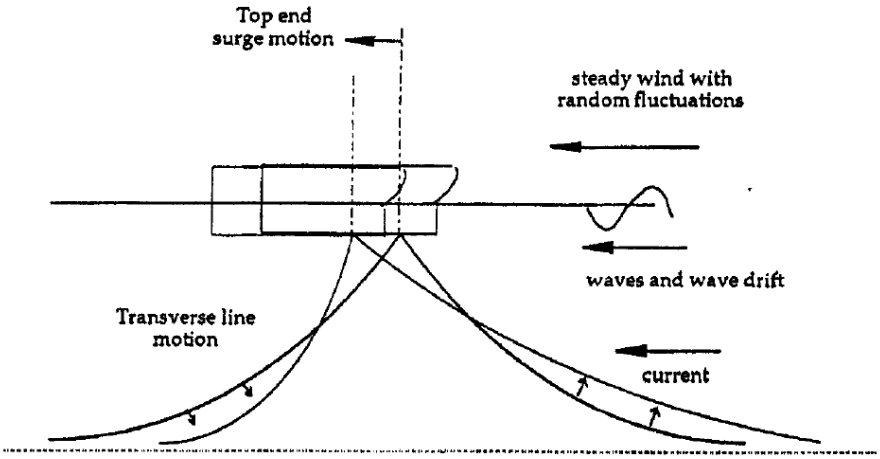

Figure 8 Environmental forces acting on a moored vessel in head conditions and transverse motion of catenary mooring lines[28]

4.1. Static Catenary Design

This is the oldest method in mooring analysis, but still most common use for preliminary design. For spread mooring system, mooring lines are modeled by catenary equation. The assumptions of this method are horizontal seabed, neglect bending stiffness and the cable is in a vertical plane coinciding with x-z plan[8]. The assumption of neglecting bending stiffness is agreed for chain, but it's also good for wire since the curvature is small. The catenary model of single line

mooring and the force acting on a segment of mooring line is depicted on Figure 9 and Figure 10 respectively.

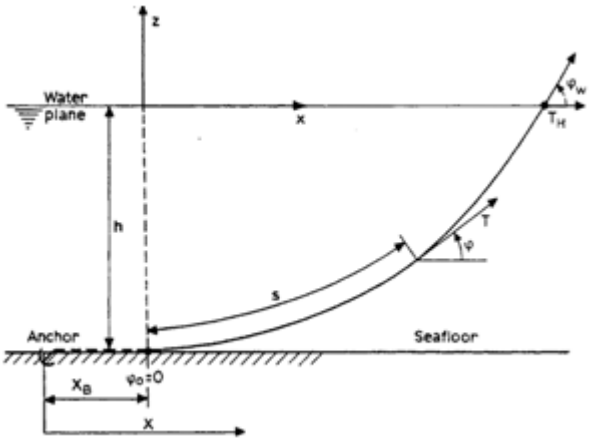

Figure 9 Cable Line and Symbols[8]

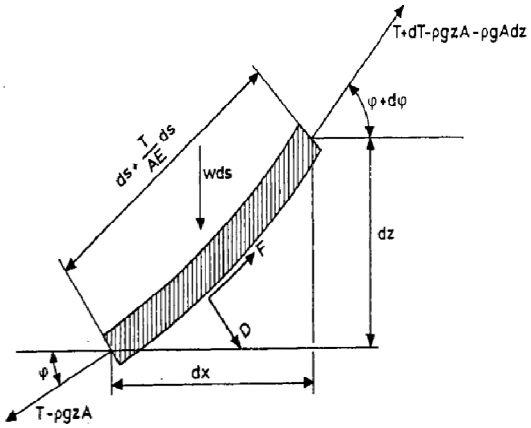

Figure 10 Forces acting on an element of mooring line[8]

Here, w is submerged weight per unit of length, A, E, T are cross-sectional area of the cable line, elastic modulus and line tension respectively. The derivation below refer to [8]. By analyzed the equilibrium in normal and tangential direction in one element of the mooring line, we can write equation as follow:

Equation 95

$$dT - \rho g A\, dz = \left[w \sin \emptyset - F\left(1 + \frac{T}{AE}\right)\right] ds$$

Equation 96

$$Td\emptyset - \rho gA\, z d\emptyset = \left[w\cos\emptyset + D\left(1+\frac{T}{AE}\right)\right] ds$$

In order to solve this question we need to linearized the equations by neglect the effect from current force (F and D). Hereafter, by introducing

Equation 97

$$T' = T - \rho gzA$$

And solve the equations above, the cable line equation can be written as

Equation 98

$$T = T_H + wh + (w + \rho gA)z$$

Where h is water depth and T_H is horizontal tension in water plane area. It has maximum tension at free surfaces (z =0). And, the vertical tension is

Equation 99

$$T_z = ws$$

We can also calculate the minimum length of the mooring lines by follow the requirement that a gravity anchor does not allow to carry vertical load.

$$l_{min} = h\left(2\frac{T_{max}}{wh} - 1\right)^2$$

And the distance between the anchor and the top of the mooring line is know by

$$X = l - h\left(1 + 2\frac{a}{h}\right)^{\frac{1}{2}} + a\, cosh^{-1}\left(1+\frac{a}{h}\right)$$

Where $a = \frac{T_H}{w}$.

Using the equation above, the forces exerted on the vessel in each catenary line can be found. It is represent the average wave, current and wind forces. The horizontal force is plotted as a function of static offset and the slope from the curve represent the restoring coefficient[28]. If the elasticity of the mooring line is considered, the equation can be found in [8] chapter 8.

The restoring force from the mooring system is found by summed the horizontal and vertical force from all mooring lines. Further, the restoring forces and tension in most loaded line is then calculated by give predetermined displacement from initial position in each direction[28].

4.2. Quasi-Static Design

It is the higher analysis of mooring line. The offset from the mooring line is determined from the analysis of the floating structures. There are two types of analysis i.e. time domain simulation and frequency response method[28]:

- Time domain simulation
  The load acting is from wave induce vessel force at wave and drift frequency, steady current and wind forces. The stiffness coefficient is found as the way in static analysis and without considering the line dynamics.
- Frequency response method
  The mooring stiffness curved is treated as linear from wave force and dynamic from wave drift and wind gust.

4.3. Dynamic Design

Full dynamic analysis is usually performed in design. This method considers the line dynamics effect when calculating the restoring forces of the vessel. The line dynamic effect comes from damping and inertial effect between the line and the fluid. The simulation used is finite element or finite difference in a small segment of the line[28].

The study of dynamics behavior of mooring lines is done by [32]. By assumes that the wave frequency motions on the structure and the mooring line can be treated separately. The mathematical model used is modification of Lumped Mass Method (LMM) in two dimensions and the equation of motion is solved in time domain. The results were the dynamics behavior strongly increase the maximum line tension and may affect the low frequency motions of the virtual stiffness and damping of the system.

4.4. Coupling Line

In condition where two bodies is connecting to the other body by coupling line, and then the motion of each body will influence to the other body. In SIMO, the simple wire coupling is modeled as a linear spring[29].

Equation 100

$$\Delta l = \frac{T}{k}$$

Where, Δl is elongation, T is wire tension, and k is effective axial stress. The effective axial stress can be found by

Equation 101

$$\frac{1}{k} = \frac{1}{EA} + \frac{1}{k_0}$$

Where $\frac{1}{k_0}$ is connection flexibility, E is modulus of elasticity and A is the cross section area.

By knowing the elongation of the end of each line, therefore the elongation and then tension are able to be determined. If the material damping is conserved, then it's included as

Equation 102

$$F = \frac{C_w \Delta l}{l \Delta t}$$

4.5. Multiple Wire Coupling

When the coupling line is connecting more than one other body, the multiple wire coupling is used. All wire segments will have one end fastened in a body and on the branch point. The axial stiffness of each wire is found by the same formula as single wire coupling. But, to determine the branch point location the iteration is needed[29].

CHAPTER V MULTI-BODY ANALYSIS IN REGULAR WAVES

This chapter describe the single body and multi-body analysis in regular waves. The purpose of the analyses are to determine the hydrodynamic coefficients and exciting forces of the floating body model i.e Cylindrical FPSO and LNG Shuttle tanker in regular waves. Here, the hydrodynamic interaction between those two bodies is also studied. The frequency domain analysis was performed in freely floating condition, no mooring line was considered.

The analysis has been performed in WADAM based on 3D Potential Theory. There are two main steps in the analysis. First, single body analysis was performed in order to obtain the response of the FPSO alone as well as LNG Shuttle tanker. Second, multi-body analysis was carried out by placing FPSO and LNG shuttle tanker side-by-side with 5 m distance. Based on the result of those two steps, then the hydrodynamic interaction may be able to be observed.

The hydrodynamic interaction on the structures was found by comparing the coefficient of added mass, damping and the transfer function of exciting forces from single and multi-body analysis results. Further, the result from the analysis i.e. hydrodynamic coefficients, exciting forces and mean drift forces transfer function later on will be used to perform time domain simulation which includes the second order waves and mooring systems.

5.1. Model Data

The FPSO model data used in the analysis is Sevan 1000 which is a cylindrical hull type of structure. Where, it was provided by Sevan Marine ASA. The principle dimensions of the FPSO are listed in the Table 1 below.

Table 1 Principle dimensions of Sevan 1000 FPSO

Description	Unit	Value
Diameter of Main Hull	m	90
Diameter of Pontoon	m	96.45
Draft	m	27
Mass	tonnes	182500
Radius of gyration in roll	m	28.5
Radius of gyration in pitch	m	28.5
Radius of gyration in yaw	m	42
Vertical centre of gravity above keel, KG	m	22.85

And, the principle dimension of LNG shuttle tanker is listed in Table 2 below.

Table 2 Principle dimensions of LNG Shuttle tanker

Description	Unit	Value
Length b/w Perpendicular	m	194
Breadth	m	38.4
Draft	m	12
Mass	tonnes	71841.1
Depth	m	18.6
Radius of gyration in roll	m	13.44
Radius of gyration in pitch	m	58.2
Radius of gyration in yaw	m	58.2
Vertical centre of gravity above keel, KG	m	11.2

5.2. Modeling Concept in WADAM

WADAM is a general analysis program for the calculation of the wave force acting on fix and floating structures[7]. In the floating structure analysis, there are two models needed during the analysis i.e. hydro model and mass model. Hydro model is used to calculate hydrodynamic forces on the structures. While, mass model is used to reports the imbalance condition between weight and buoyancy and used for solving equation of motion.

Hydro model that used for large volume body is called panel model. The Input Interface File of the panel model is generated from GENIE (3D modeling software owned by DNV)[33-34]. The wet surface on the panel model is represented by the dummy load on the panel model.

An important note to be notice during this step is the consideration of the coordinate system. As explained in sub-chapter 2.1 that there are difference coordinate system used in single body and multi-body analysis. In multi-body analysis, the results refer to body coordinate system. While, in single body analysis it refers to global coordinate system. The mistake on this step will tend to significant error in the further analysis.

Figure 11 below presents the multi-body model established in WADAM.

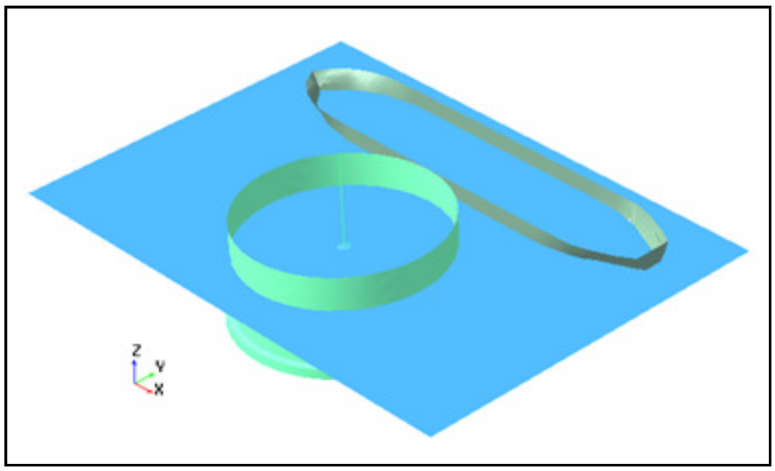

Figure 11 Multi-body model in WADAM

5.3. Multi-body Analysis in WADAM

Single body and multi-body analysis has been performed in 300 m water depth. The regular waves variation is defined by varying wave period from 3 – 30 s. The incoming wave direction is also varied from 0^0-360^0 in interval of 30^0. In WADAM, it is also possible to specified the viscous damping by input the additional damping matrix.

During the analysis WADAM will computes mass and restoring force from hydrostatic calculation. While the added mass, potential damping and the exciting force is calculated based on 3 Dimensional Potential Theory. Furthermore, the results will be discussed in the next sub-chapter.

5.4. Added Mass and Potential Damping

As explained in sub-Chapter 2.3.2, that the present of LNG Shuttle tanker will affect the hydrodynamic force acting into FPSO, and vice versa. In the radiation problem, the presence of the hydrodynamic interaction between FPSO and LNG Shuttle Tanker can be revealed from the added mass and potential damping coefficients. Both added mass and potential damping are frequency dependent.

For clearer explanation here will be presented the added mass and total damping in some degree of freedoms of FPSO and LNG Shuttle tanker. Figure 1 below shows the added mass of FPSO in sway and heave motion. The red curve presents the added mass coefficient of single body FPSO. While, the blue curve presents the added mass coefficient when it is analyzed together with the LNG shuttle tanker (multi-body).

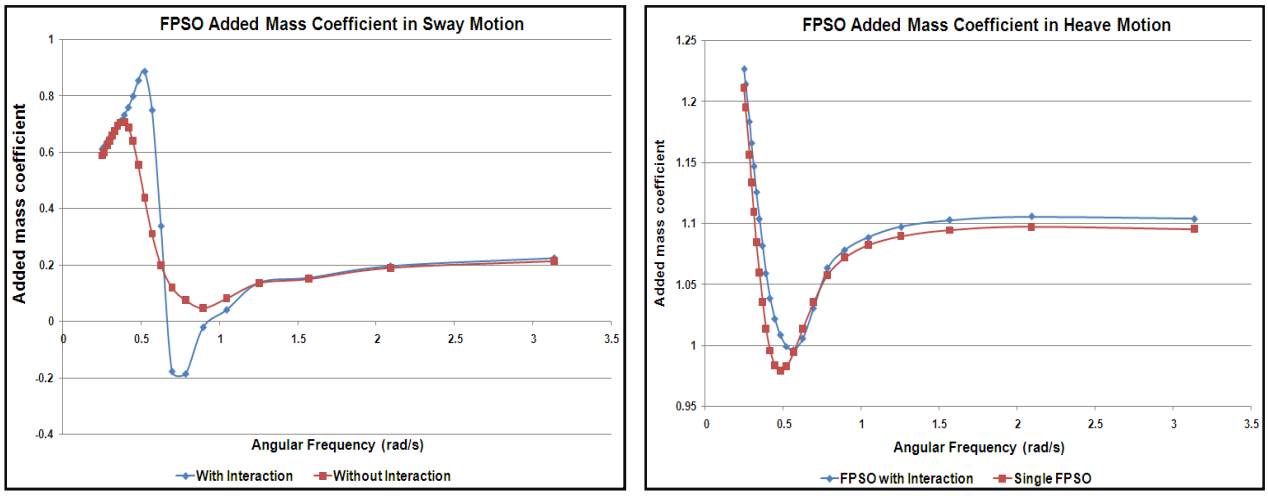

Figure 12 FPSO Added mass coefficients in sway and Heave Motion

From the comparison between blue and red curve, the influence of hydrodynamic interaction in added mass is clearly shown. The result shows that in all frequencies, except in the range of 0.571 rad/s – 0.698 rad/s added mass of FPSO in heave is increased due to the presence of the LNG Shuttle tanker. Decreasing added mass coefficient in frequency range 0.571 rad/s – 0.698 rad/s is come from the negative value of FPSO – LNG Shuttle tanker coupling added mass. Similar with heave, in sway motion it also results the negative added mass coefficient. Figure 13 shows the FPSO – LNG Shuttle Tanker coupling added mass in sway and heave motion.

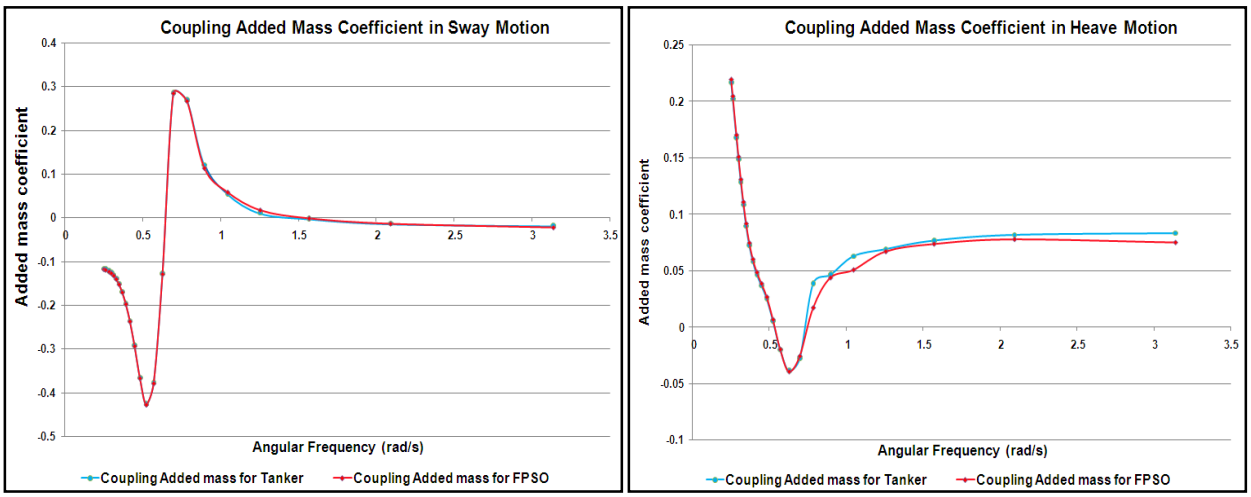

Figure 13 FPSO – LNG Shuttle Tanker coupling added mass in sway and heave motion

For LNG Shuttle Tanker, presence the FPSO decreases the added mass in sway and yaw motion. It's agree with the study of hydrodynamic interaction between two ship advancing in waves done by Fang et al. (2000) [15].

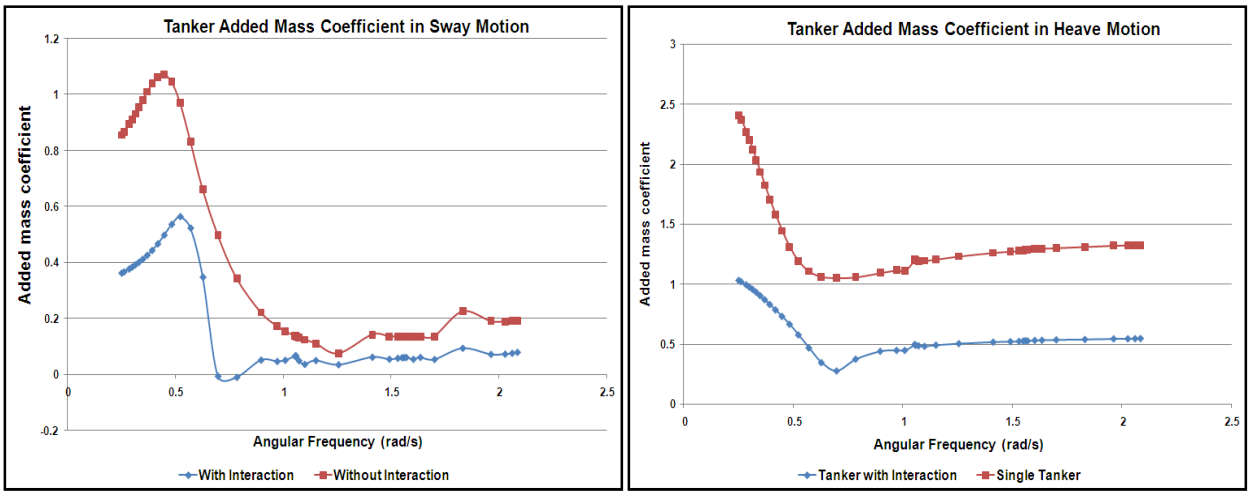

Figure 14 Tanker Added mass in sway and Heave Motion

Figure 15 shows the FPSO total damping in sway and roll motion. The total damping consists of potential damping and specified damping matrix. The specified damping matrix is provided by Sevan Marin ASA. For FPSO, the specified damping matrix is inputted. Then, it leads to non-zero damping in roll motion for very long and very short wave. If only potential damping is considered then the damping coefficient in very long and very short wave is almost zero.

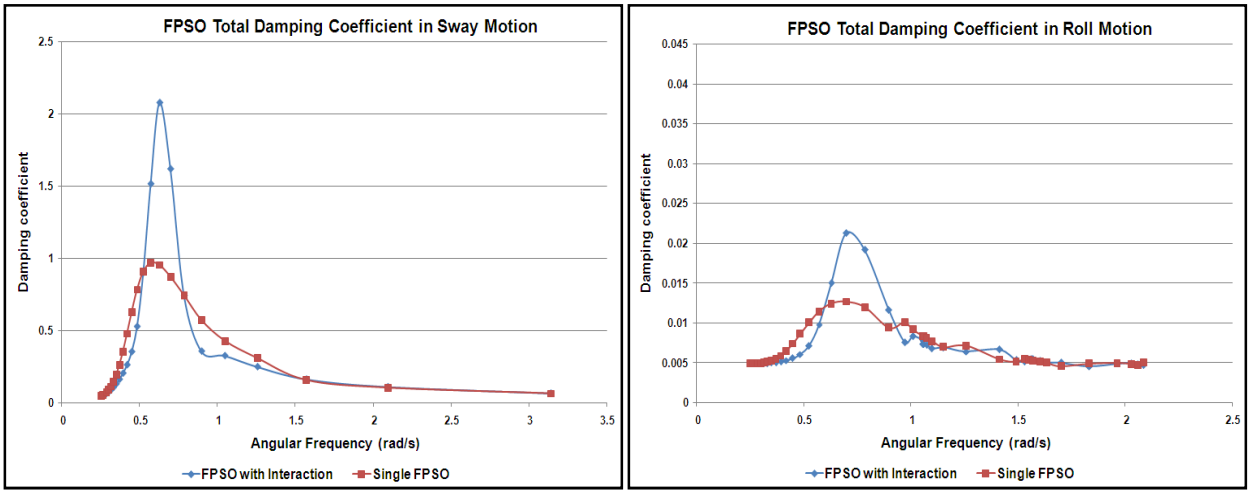

Figure 15 FPSO Total damping Coefficient in Sway and Roll Motions

From the comparison between FPSO analyzed as single body and multi-body, it shows that the hydrodynamic interaction increase the potential damping around the resonance frequency.

For LNG Shuttle tanker in sway and heave motions, damping coefficient for single-body has larger value than multi body. This also agrees with the result from Fang et al. (2000) [15].

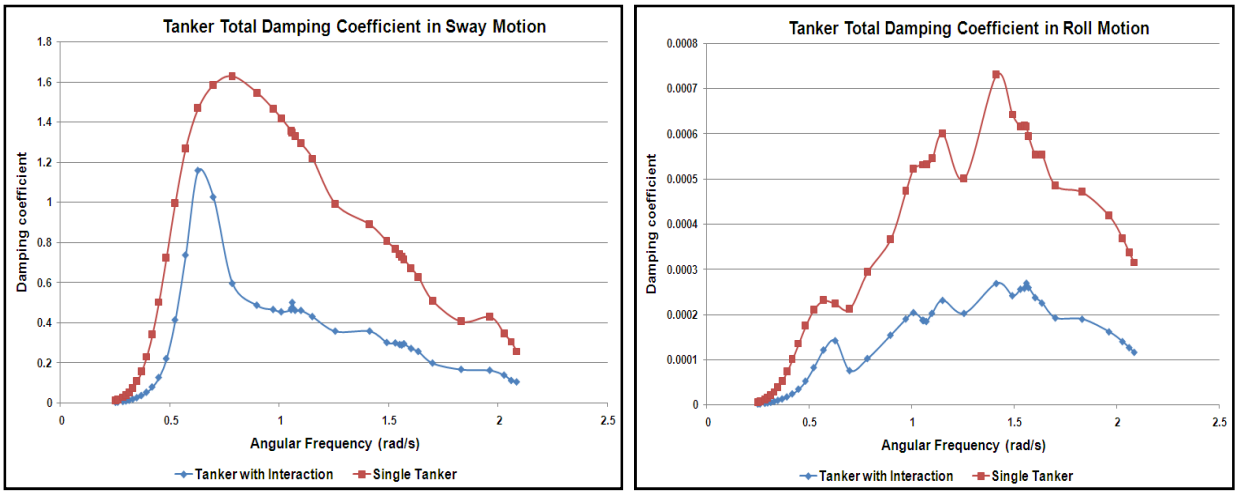

Figure 16 Tanker Total damping Coefficient in Sway and Roll Motions

5.5. Excitation Forces

Similar way with radiation problem above, the hydrodynamic interaction effect is also presence in the diffraction problem. The hydrodynamic interaction can be shown from wave frequency forces and mean drift forces.

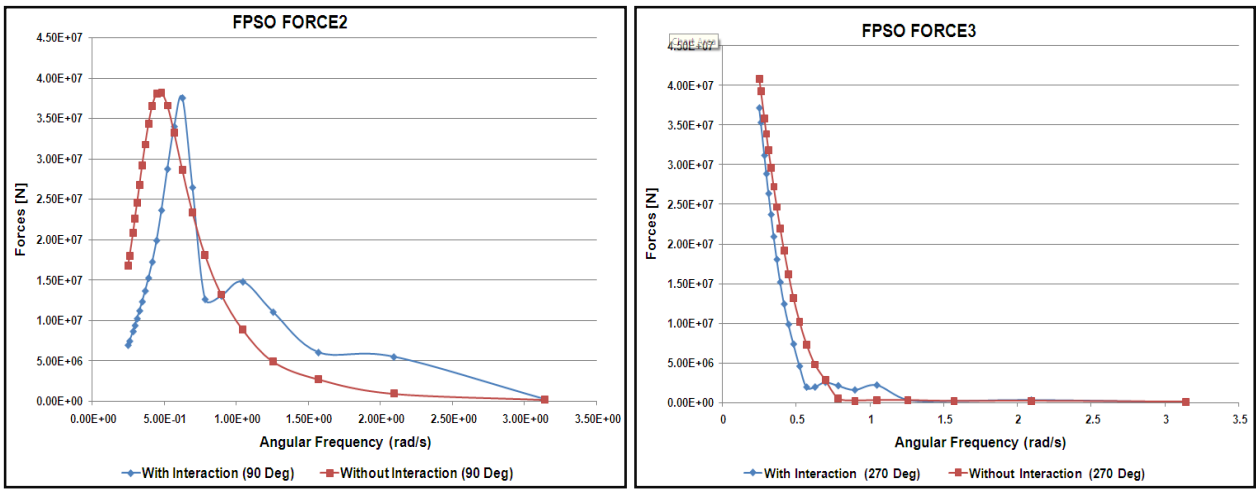

Figure 17 First order wave force in X(FORCE2) and Y(FORCE3) propagating directions (FPSO)

Figure 17 below shows the wave frequency forces acting to the FPSO in sway and heave motions. The results show that the multi-body has smaller value in long wave compare to the single body. While in short waves the wave frequency force is increased.

While for tanker, increasing force in heave occurred in frequency range 0.524 rad/s -0.898 rad/s for sway motion. For heave motion it's occurred in frequency below 0.0571 rad/s. It's shown at Figure 18.

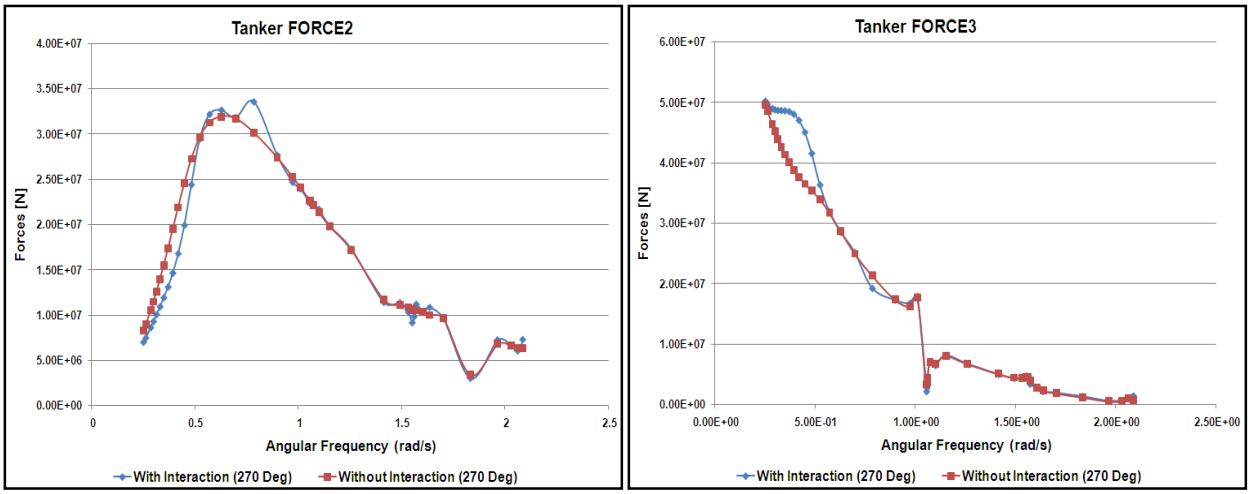

Figure 18 First order wave force in X(FORCE2) and Y(FORCE3) propagating directions (Tanker)

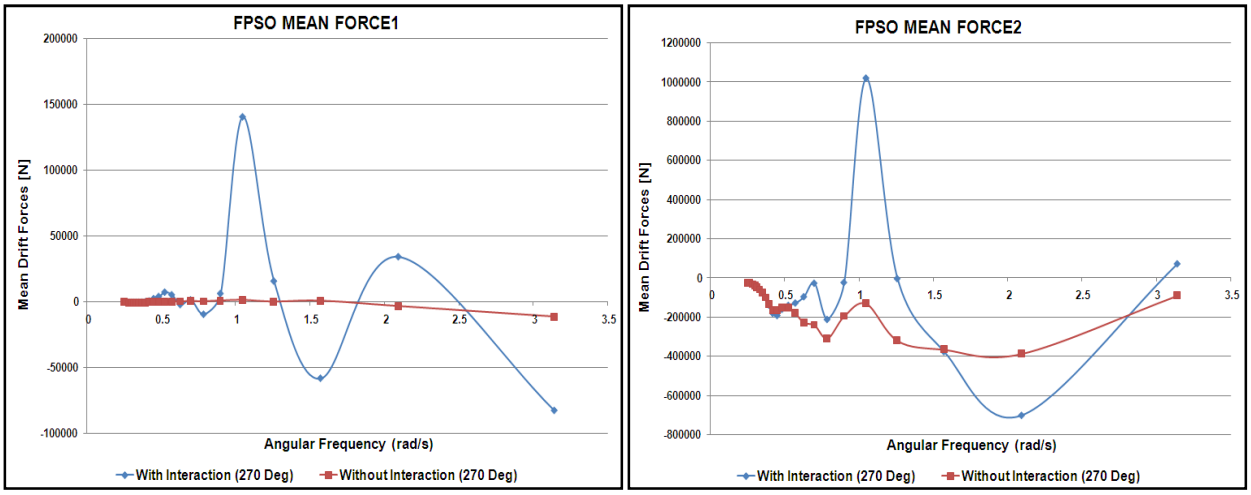

Figure 19 FPSO Mean Drift Forces in 270^0 incoming waves

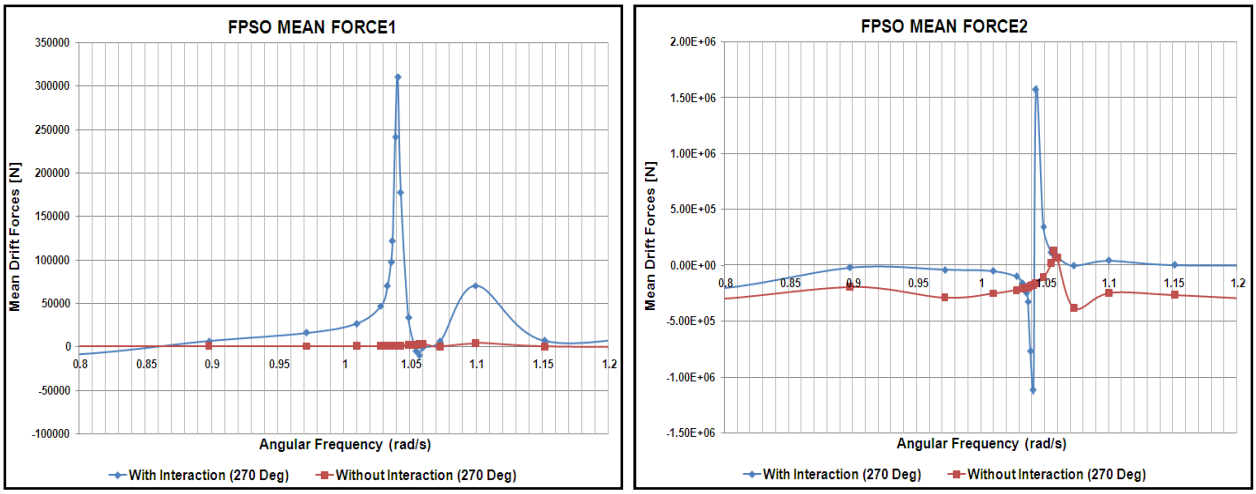

Figure 20 FPSO Mean Drift Forces in 270^0 incoming waves

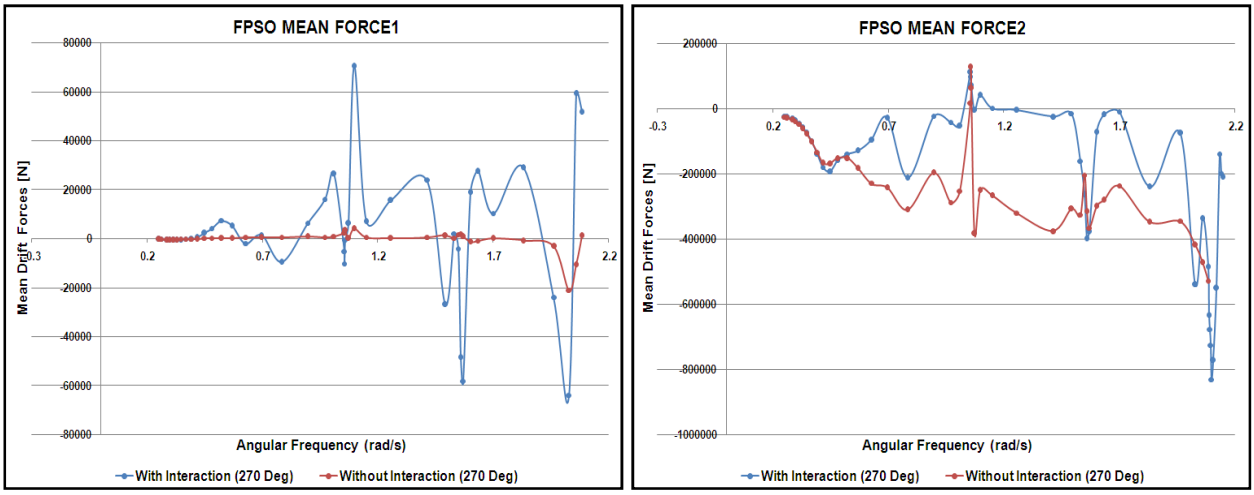

Figure 21 FPSO Mean Drift Forces in 270^0 incoming waves

Instead of the wave frequency force, here is also interesting to study the hydrodynamic interaction influences the mean drift forces.

From Figure 19 shows that the hydrodynamic interaction has very large influences to the wave drift force. If we look carefully the peak value it seems unreasonable. The biggest mean drift force is 1.2E+106 N. It's very large compare with the mean drift force in the other directions. The reason is it might be contain the numerical error.

To observe this problem, the second running has been taken by adding denser frequency around the peak i.e. 1.047 rad/s. The result is shown as Figure 20. It's clearly shown that it's found the numerical error. The mean drift force jumps significantly in very small neighboring frequency (1.028 – 1.049 rad/s). After put denser frequency around 1 rad/s – 1.2 rad/s and exclude the frequency 1.047 rad/s then the correct result is found.

Figure 21 shows that considering the hydrodynamic interaction will produces both positive and negative mean drift force in FPSO. It means that the negative mean drift force is produced from the reflection wave due to the presence of LNG Shuttle Tanker.

For LNG Shuttle tanker, the hydrodynamic interaction will increase the mean drift force. The comparison of mean drift force in surge and sway motion are shown in Figure 22 below.

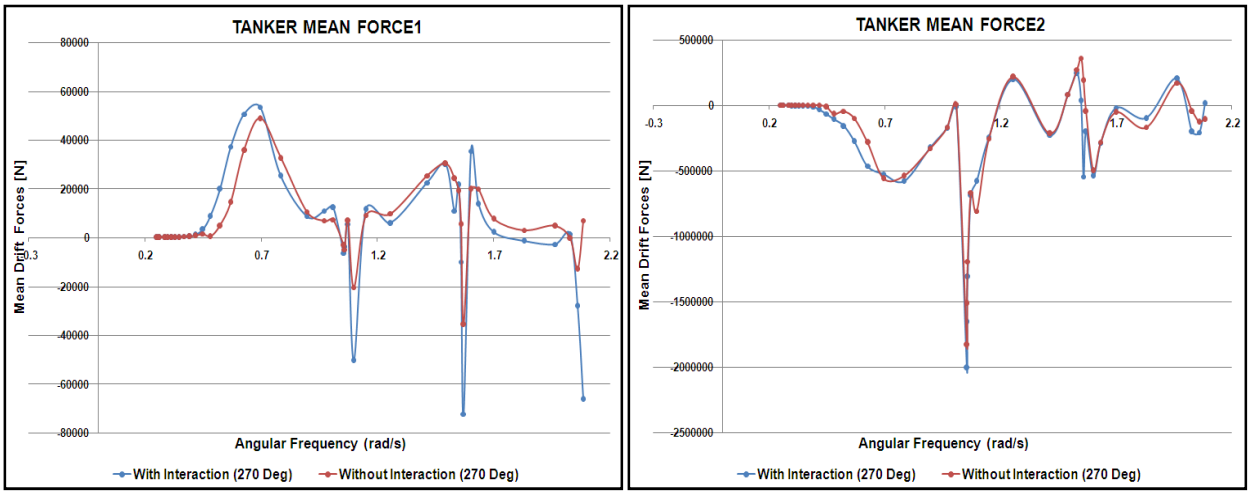

Figure 22 Tanker Mean Drift Forces in 270^0 incoming waves

CHAPTER VI OFFLOADING SYSTEM IN IRREGULAR WAVES

This chapter focused on the analysis of the offloading system performance in varying sea-state. Here it is also studied the hydrodynamic interaction influence in the offloading system. Not only the wave load, wind and current are also considered in to the analysis. The step of the analysis consists of three parts, i.e. Static Equilibrium analysis, Decay Test and Time Domain simulations. All analyses are performed in SIMO.

Prior performing time domain analysis in SIMO, we need information for hydrodynamic coefficient and the exciting forces in regular waves. The information are is imported from previous analysis in WADAM. Since the results are frequency dependent, therefore the transformation is performed in INPMOD. INPMOD solved the transformation process by using convolution integral. More detail information refers to sub-Chapter 3.3.1.

6.1. Side-by-side Offloading Configuration

The LNG offloading configuration is the modification from the previous study of offloading system applied for oil offloading process[5]. The Offloading system is designed for 300 m water depth. The mooring system for FPSO consists of 12 mooring lines which are attached into three points. The mooring line characteristics of FPSO are listed as Table 3 below. Sketch of the Offloading configuration is shown as Figure 23.

Table 3 FPSO Mooring Line Characteristic

Segment type (from anchor)	Length (m)	Nominal diameter (m)	Elastic Modulus E (kN/m^2)	Weight in air (kN/m)
Lower Chain	350	0.178	0.46E+08	6.218
Rigid Link	2	0.178	1.00E+08	500
Polyester Rope	1000	0.290	0.76E+07	0.556
Upper Chain	125	0.178	0.46E+08	6.218

Whereas LNG Shuttle tanker has 2 mooring lines in bow and aft, 2 spring lines connected to the FPSO, 2 back up lines connected to buoy and catenary line from the buoy to the anchor. The mooring lines are

modeled as catenary. While, coupling lines and back up lines are modeled as linear force-elongation relationship. Table 4 below is the FPSO mooring line orientation relative to the local coordinate system.

Table 4 FPSO Mooring Line Orientation

Line No.	Local direction (degree)
1	308
2	306
3	294
4	292
5	188
6	186
7	174
8	172
9	68
10	66
11	54
12	52

Table 5 Tanker Mooring Line Characteristic

Segment type (from anchor)	Length (m)	Nominal diameter (mm)	Axial Stiffness (kN)	Weight in air (kN/m)
Tanker Mooring Lines (L1 andL2)				
Bottom chain	35	0.076	4.650E+05	1.160
Polyester Rope	280	0.120	8.680E+04	0.100
Dyneema Chain	713	0.068	8.000E+04	0.032
Coupling Line connected to FPSO (L3 and L4)				
Polyester Rope	57.72	0.095	0.544E+05	0.06
Back up Line (L5f and L5a)				
Dyneema Chain	703	0.068	0.800E+05	0.032

The minimum axial stiffness is estimated by:

- Polyester EA = 20 . MBL
- Dyneema EA = 20 . MBL

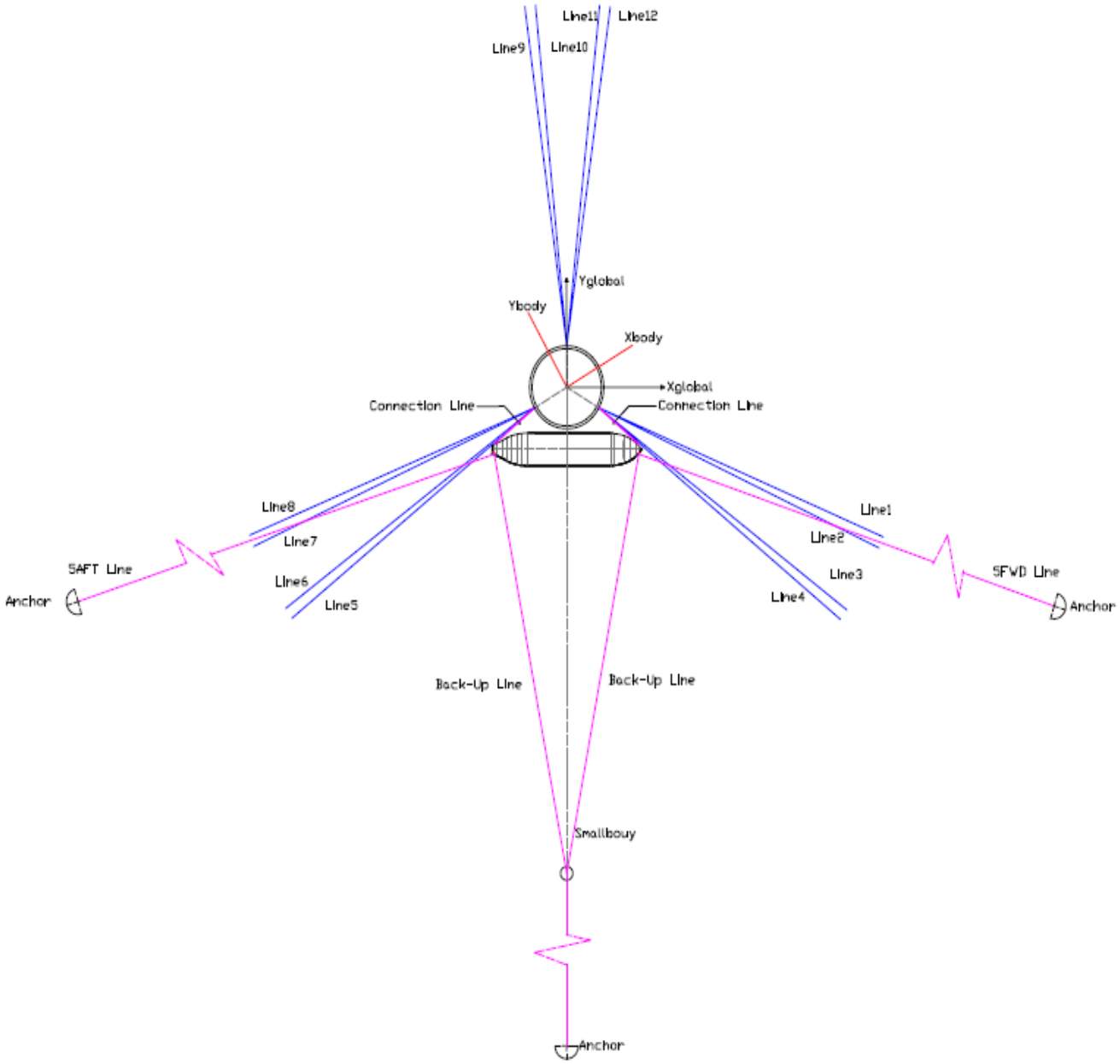

Figure 23 Side-by-side Offloading Configuration of FPSO and LNG Shuttle Tanker

6.2. Static Equilibrium

The equilibrium condition of the multi-body system is found by stepping the equation of motion. From static equilibrium calculation in STAMOD, the initial positioning element forces and coupling element force applied on the system are listed as Table 6 below.

Table 6 Pretension of Mooring and Coupling Line

Parameter	Value	Unit
FPSO Line 1 - 8	1775	[kN]
FPSO Line 9 -12	2000	[kN]
Tanker Line 1 and 2	182	[kN]
Tanker Line 5f and 5a	383	[kN]
Coupling Line 3 and 4	757	[kN]
Buoy Line	774	[kN]

In the same configuration, equilibrium position for multi-body system without considers the hydrodynamic interaction is found after 51.2 s. While, for multi-body with interaction it is found after 204.8 s.

6.3. Decay Test

Before the processing of complete analysis of multi-body system in variation of environment condition, it needs to be convinced that both of FPSO and LNG Shuttle tanker has favorable behavior and reasonable natural period.

There are two ways to obtain natural period of the FPSO, LNG Tanker and offloading system in SIMO. Eigen value analysis in STAMOD is the simplest way to find natural period. But, it should be note that it's based on the linearized model of the system i.e. mass and stiffness are calculated and the system is solved by iterative method standard jacobian solver[29] .Here, the effect of the damping is not included in the analysis.

The second way is by performing decay test is DYNMOD. The initial displacement need to be specified as an initial condition. Then, the time domain simulation is performed without includes any external loads. Single FPSO decay test has been performed by specified the initial displacement equal to 5 m. While,

LNG Tanker decay test uses 0.5 m initial displacement. The time domain simulation is performed in 50 minutes duration. From decay test result, damped period and damping ratio can be calculated using logarithmic decrement. And after that, natural period is able to be obatained.

For offloading system, decay test was performed in two conditions i.e. with and without consider the hydrodynamic interaction. The aim is to understand the alteration of natural period due to the change of added mass. In Figure 24, 18 and 19 shows the time series of FPSO and LNG Shuttle tanker decay test in heave, surge and sway respectively.

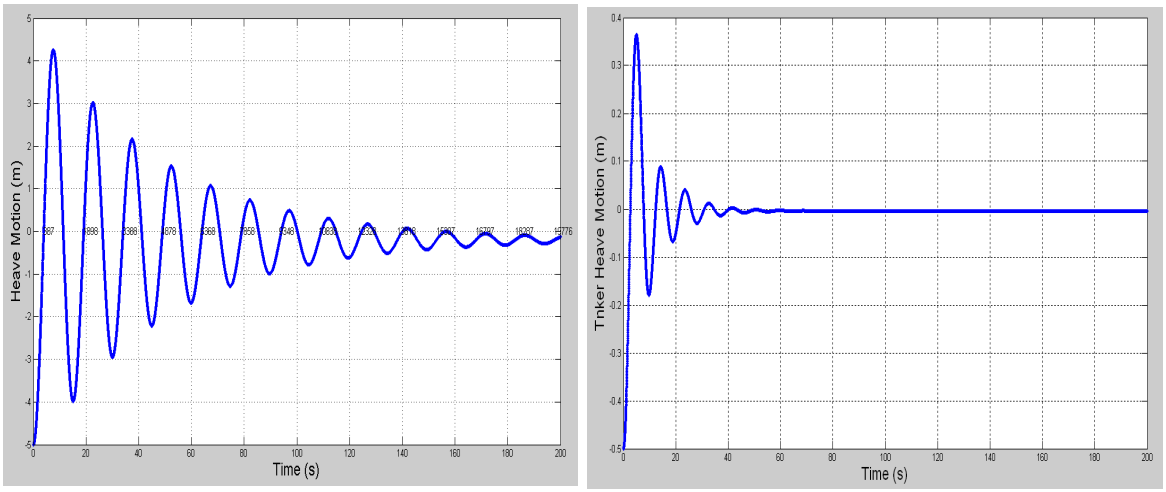

Figure 24 Single body decay test of FPSO (Left) and LNG (Right) Shuttle tanker in heave

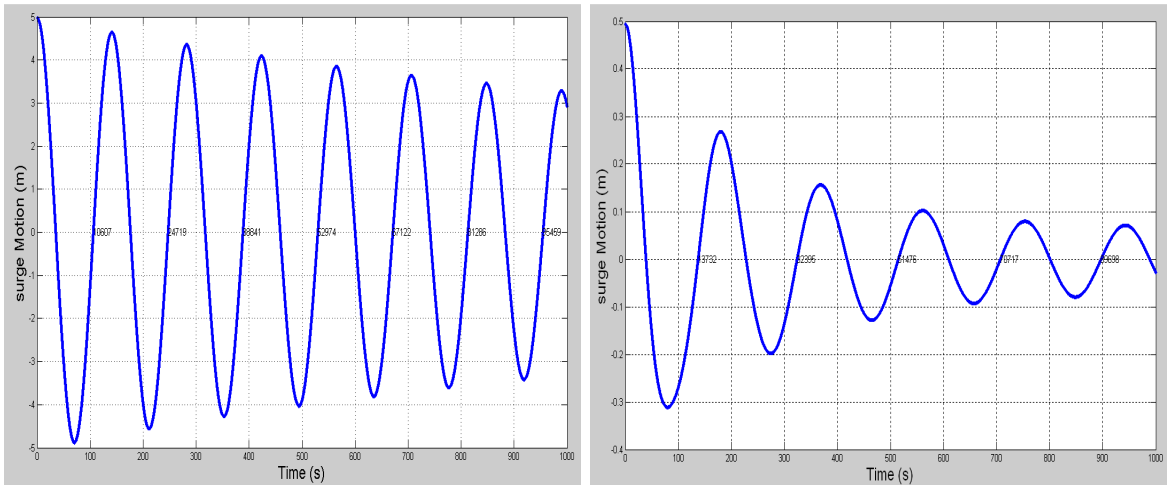

Figure 25 Single body decay test of FPSO (Left) and LNG Shuttle tanker (Right) in surge

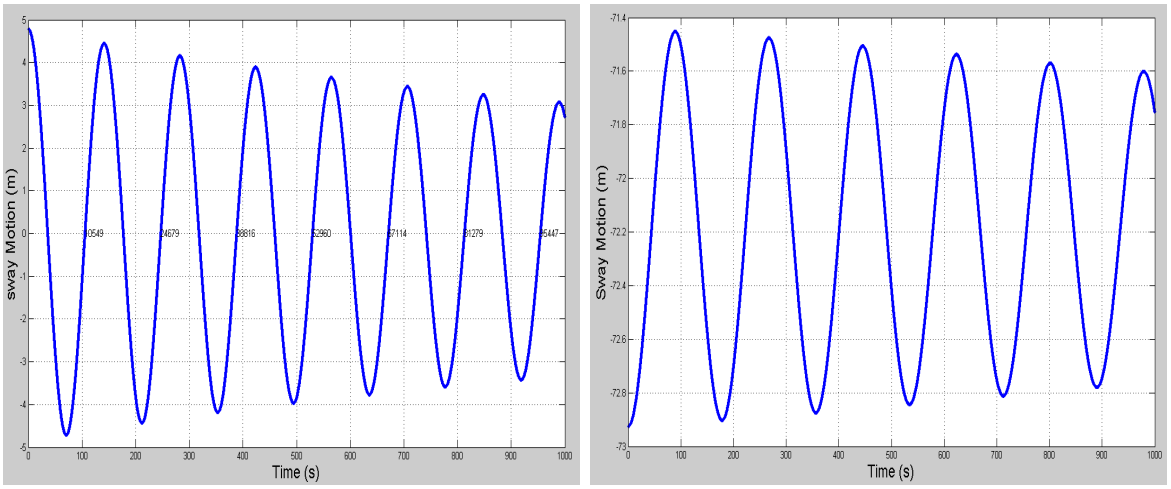

Figure 26 Single body decay test of FPSO (Left) and LNG Shuttle tanker (Right) in sway

Single FPSO decay test was modeled alone with 12 mooring lines. While, LNG Shuttle tanker decay was model as multi-body model included all mooring system and coupling line. In this configuration FPSO is kept in the fix position during the analysis.

Figure 27 shows damping ratio and damped period of FPSO in heave motion. The mean value of damping ratio and damped period is then used for natural period calculation. From the right figure (damping ratio and damping period relation) shows that the calculation gives very good result.

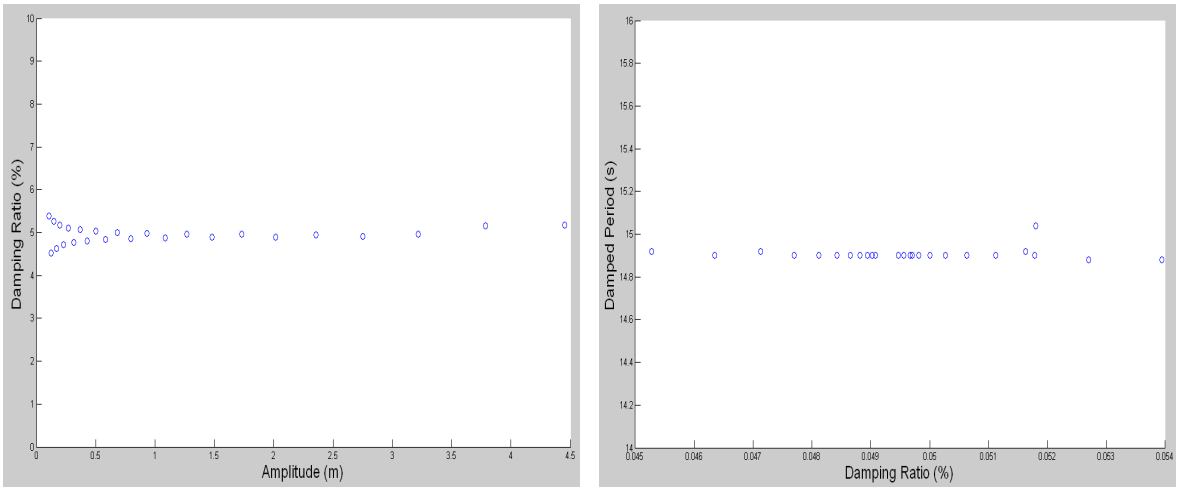

Figure 27 Damping ratio and Damping Period of Single FPSO in heave Motion

In Table 7 and Table 8 are listed the damped period and damping ratio of the system. It is shown that for larger value of damping the natural period increase.

Table 7 Damped Period from Decay test in DYNMOD

Motion	Damped Period [s]					
	Single body		Multi-body Without Interaction		Multi-body With Interaction	
	FPSO	Tanker	FPSO	Tanker	FPSO	Tanker
Surge	141.4	191.0	218.2	205.4	217.9	209.7
Sway	141.4	177.7	132.5	194.3	136.3	196.5
Heave	14.9	9.1	14.9	9.1	15.1	11.4

Table 8 Damping ratio calculated from Decay test in DYNMOD

Motion	Damping Ratio					
	Single body		Multi-body Without Interaction		Multi-body With Interaction	
	FPSO	Tanker	FPSO	Tanker	FPSO	Tanker
Surge	0.0089	0.055	0.0387	0.0427	0.034	0.032
Sway	0.0076	0.007	0.005	0.005	0.010	0.006
Heave	0.0496	0.158	0.053	0.158	0.057	0.127

Table 9 Natural Period calculatied from STAMOD

Motion	Natural Period [s]					
	Single body		Multibody Without Interaction		Multibody With Interaction	
	FPSO	Tanker	FPSO	Tanker	FPSO	Tanker
Surge	125.3	150.2	136.0	150.2	136.3	150.2
Sway	125.3	113.1	128.3	113.1	128.8	113.4
Heave	15.3	10.3	15.3	10.3	15.4	10.7

Table 10 Natural Period calculate from Decay test in DYNMOD

Motion	Natural Period [s]					
	Single body		Multi-body Without Interaction		Multi-body With Interaction	
	FPSO	Tanker	FPSO	Tanker	FPSO	Tanker
Surge	141.4	190.7	218.1	205.2	217.8	209.6
Sway	141.4	177.7	132.5	194.3	136.3	196.5
Heave	14.9	9.0	14.9	9.0	15.1	11.4

Table 9 and Table 10 are summary of natural period obtained from eigen value analysis and decay test. The result shows that natural period of surge and sway motions in Table 8 are different as compared to the ones in with Table 10. Hence, in this case it's not a good way to linearized model of the system i.e the effect of dynamic in mass and stiffness calculation need to be considered.

By comparing the natural periods in surge, sway and heave obtained from the multi-body with interaction and without interaction (Table 10), we will observe the influence of the hydrodynamic interaction influence to the natural period of the structures. Natural period of the multi-body with interaction is larger than natural period of multi-body without interaction. The reason is explained in sub-chapter 5.4. It means that hydrodynamic interaction comes from the presence of LNG shuttle tanker, which increases the added mass of FPSO, and vice versa. Thus, it increases the total mass of the structures which has proportional relation with the natural period of the structures.

6.4. Multi-body Analysis in Irregular waves

In regular waves, we have already found the influence of hydro dynamic interaction in added mass, potential damping and exciting force. In real condition, the offloading system will experience the irregular waves, wind and current with variation of combination. In this sub-chapter, the aim is to study the offloading system performance in varying sea-state and directions. The effect of wind and current are also studied. The main results which will be discussed are the exciting force and motion of the offloading system.

Time domain simulation is taken for 3 hours 38 minutes (65536 steps with 0.2 time steps). In order to avoid the influence of the transient effect, the result is analyzed for the last 3 hours. The variation of sea-state and direction of waves, wind and current are listed on the Table 11.

Table 11 List of wave, wind and current variation

Run No.	Wave				Wind and Current		
	Hydrodynamic Interaction	Hs [m]	Tp [s]	Direction [Deg]	Wind [m/s]	Current [m/s]	Direction [Deg]
1	No	2	7	180	-	-	-
2	No	2	14	180	-	-	-
3	No	3	8	180	-	-	-
4	No	2	7	270	-	-	-
5	No	2	14	270	-	-	-
6	No	3	8	270	-	-	-
7	Yes	2	7	90	-	-	-
8	Yes	2	14	90	-	-	-
9	Yes	2	7	180	-	-	-
10	Yes	2	14	180	-	-	-
11	Yes	2	7	270	-	-	-
12	Yes	2	14	270	-	-	-
13	Yes	0.5	4	270	-	-	-
14	Yes	0.5	4	270	10	-	270
15	Yes	0.5	4	270	10	1	270
16	Yes	2	14	270	10	-	270
17	Yes	2	14	270	10	1	270
18	Yes	2	14	270	10	1	180

6.4.1. Frequency Wave Forces and 2nd Order Wave Forces

Prior continuing the discussion, it's good to understand how much the wave energy contain in difference significant wave height (Hs) and peak period (Tp). By observing the wave elevation time series generated from Run No. 1-3 and then transforms it in to wave spectrum, the result shows that the increasing Hs and/or Tp will produce significant increase of wave energy.

In the first part will be studied how the wave frequency force and wave drift force acting on the structures due to increasing sea-state. Running no 1-3 in Table 12 has been performed in multi-body model without included the hydrodynamic interaction.

In Table 12 below, the running result of wave frequency forces and second order wave forces acting on FPSO in varying condition (Table 11) is presented as statistical properties mean and standard deviation.

Table 12 Wave frequency forces and Second order wave forces acting on FPSO

Run No.	1st order wave forces [kN]						2nd order wave forces [kN]			
	Fx		Fy		Fz		Fx		Fy	
	Mean	Std	Mean	Std	Mean	Std	Mean	Std	Mean	Std
1	0.0004	5141.1	0.0011	2960	2.52E-05	450.53	-108.07	108.82	62.83	63.27
2	0.0072	13641.0	0.0043	7870	2.88E-05	6940.6	-76.99	78.35	44.47	45.26
3	0.0024	10478.0	0.0039	6042.4	2.73E-05	1409.7	-239.39	237.48	138.88	137.8
4	-0.0006	2967.0	0.0024	5132.2	-7.05E-06	455.36	-62.21	62.64	-109.18	109.97
5	-0.0040	7878.4	0.0035	13655	-1.89E-05	6959.2	-44.50	45.30	-77.89	79.30
6	0.0207	6052.9	0.0134	10437	-7.257E-05	1418.5	-137.97	137.04	-240.29	238.45
8	0.0175	9635.6	-0.0059	13342	-2.680E-04	8698.6	47.45	48.53	67.89	69.37
9	0.0002	4780	-0.0026	6015.1	5.51E-04	725.11	-143.66	144.82	-81.05	99.61
10	0.0428	15869	0.0307	8015.1	-0.92E-03	8449.7	-86.02	87.29	4.88	45.99
12	0.0079	6818.6	0.0040	9520.7	3.39E-05	5098.6	-36.40	37.43	-54.88	57.92
13	-14.57E-09	44.6	6.33E-07	63.61	-3.41E-07	17.99	0.14	0.85	1.64	1.65
14	2.413E-05	44.58	-8.52E-06	63.61	2.24E_06	17.97	0.13	0.85	1.63	1.64
15	2.97E-05	43.91	2.68E-05	63.74	-2.46E-05	17.61	0.13	0.84	1.47	1.54
16	-0.0026	6816.4	-6.15E-04	9520.8	-0.0026	5098.3	-36.38	37.41	-54.88	57.92
17	0.0248	6720.7	-0.141	9512.4	-7.55E-04	5089.3	-35.79	36.84	-54.82	58.03
18	-0.016	6828	0.0027	9519.5	5.75E-04	5100.5	-36.48	37.50	-54.86	57.89

The comparison is taken from running no 1-3 in Table 12 above. It shows that in the long wave (Run No. 2) force acting on FPSO are dominated by wave frequency force. In this condition, the vertical force increase significantly along with increasing Tp. While in shorter wave (Run No.1), second order forces are more dominant. In Run No. 3, there is combination of wave frequency forces and second order forces. For tanker, the vertical component of wave frequency force is most dominant. While, second order wave force is not too high compare to FPSO. It is because of the small projected area attacked by 180^0 incident wave.

The second part is study of wave frequency force and second order wave force acting on the structures in varying incident wave direction. For comparison, incident wave 180^0 (Run No. 2) and 270^0 (Run No. 5) are taken. Due to the symmetrical shape of FPSO, there is only small difference force acting on 180^0 and 270^0 incident waves. It is the same with the vertical component of wave frequency forces. Incident wave 270^0 produces vertical forces slightly higher than 180^0.

While for tanker the incident wave 270^0 produces large forces both in wave frequency force and second order forces. It can be shown in Table 13 Run No. 2 and 5.

Table 13 Wave frequency forces and Second order wave forces acting on Tanker

Run No.	1st order wave forces [kN]						2nd order wave forces [kN]			
	Fx		Fy		Fz		Fx		Fy	
	Mean	Std	Mean	Std	Mean	Std	Mean	Std	Mean	Std
2	0.0096	2198.1	0.3102	24.11	0.014	8318.7	-25.04	24.79	0.097	0.341
5	0.3477	331.71	-0.7959	13317	0.3176	16201	4.385	5.777	-199.32	199.32

6.4.2. Influence of Hydrodynamic Interactions

Continuing from previous sub-chapter, here we will discuss the influence on wave frequency force and drift force acting on the multi-body system when hydrodynamic interaction is taken into account. Running No. 7-12 in Table 12 has been performed in order to get understanding of interaction effect on varying sea-state and wave direction.

Similar with the previous sub-chapter, the study of hydrodynamic interaction aims two objectives. First, to understand the hydrodynamics interaction effect due to increasing sea-state. Secondly is to know the hydrodynamics interaction in variation of direction.

Based on the running result No 1,2,9, 10 in Table 12, it's concluded that hydrodynamic interaction endorses the increasing wave frequency force along with the increasing sea-state. It's explained as below.

By comparing the result for horizontal force in running no. 1 and 2 (without hydrodynamic interaction) the increasing force is 8500 kN, while by comparing the result from running no. 9 and 10 (with hydrodynamic interaction) the increasing force becomes 11089 kN.

In addition, the effect of hydrodynamic interaction can be shown from the second order wave force. For se-state Hs = 2m, Tp = 14 s and wave direction 180 Deg, the wave drift force acting in y direction of FPSO is generated in positive directions i.e away from FPSO and tanker. Meanwhile, when hydrodynamic interaction is considered the wave drift force will be generated in both positive and negative y directions. It means that there is also wave drift force generated from the tanker acting to the FPSO. It is shown in Figure 28 below.

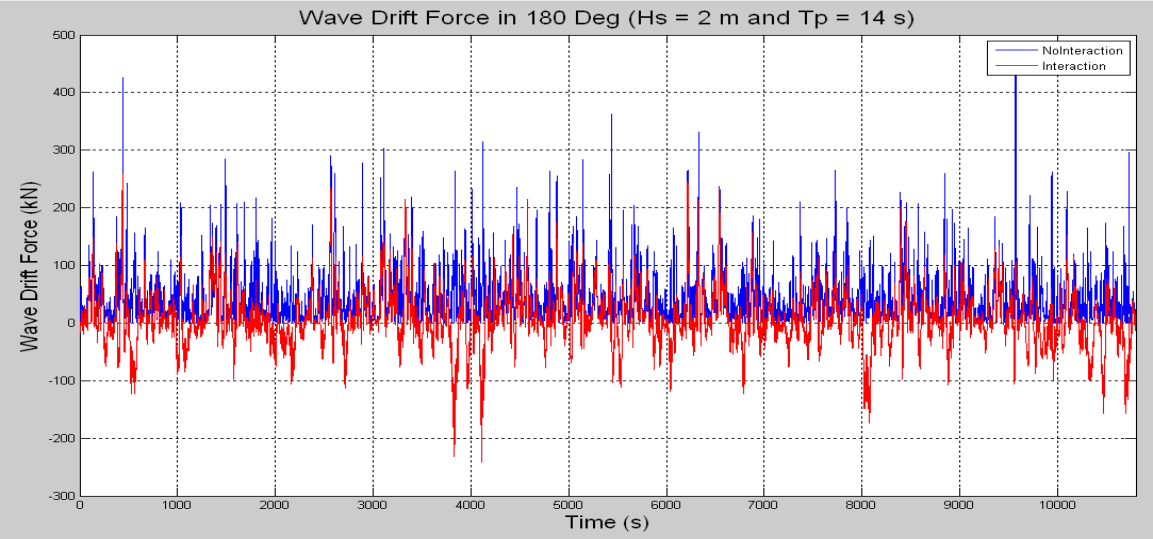

Figure 28 FPSO Wave Drift Force in 180 Deg (Hs=2m, Tp=14s)

Different incident wave direction will give different effect of hydrodynamic interaction. Here, the comparison is taken between running No.2 and 10 for 180^0 incoming waves and running No.5 and 12 for 270^0. From the result listed on Table 12 concluded that in 180^0 incoming waves both the wave frequency forces and second order wave force increased when the hydrodynamic interaction is considered.

6.4.3. Effect of Wind and Current

Instead of wave, wind and current loads are also need to be considered in moored structure analysis. In this part, the contribution of the wind and current forces to the total forces acting on the FPSO and LNG tanker will be discussed.

By reviewing the result from running No. 13, 14, 15, it shows that in low sea-state the presence of wave and current gives small influence in the global forces.

6.5. FPSO and LNG Shuttle Tanker Motion

The discussion in previous sub chapter give basic understanding of the wave, wind and current force acting to the multi-body system along with the hydrodynamic interaction. Further, here will be discussed the motion of the offloading system.

In Table 14 below summarize the statistical properties of motion for FPSO and LNG Shuttle tanker in varying loading conditions.

Table 14 FPSO and LNG Shuttle Tanker motions

Run No.	FPSO Motion [m]						LNG Shuttle Tanker[m]					
	Surge		Sway		Heave		Surge		Sway		Heave	
	Mean	Std	Mean	Std	Mean	Std	Mean	Std	Mean	Std	Mean	Std
1	-0.349	0.297	-0.008	0.118	-0.189	0.031	-0.519	0.297	-72.253	0.118	-0.003	0.031
2	-0.262	0.426	-0.010	0.073	-0.189	0.659	-0.456	0.426	-72.246	0.073	-0.003	0.659
3	-0.819	0.859	-0.023	0.138	-0.189	0.039	-1.375	0.859	-72.316	0.138	-0.003	0.039
4	-0.138	1.208	-1.456	3.989	-0.192	0.031	0.022	1.208	-81.606	3.989	-0.001	0.031
5	0.0004	0.175	-0.365	0.910	-0.190	0.659	0.092	0.175	-73.698	0.910	-0.003	0.659
6	-0.127	1.852	-2.653	4.897	-0.194	0.039	0.494	1.852	-88.271	4.897	-0.0004	0.039
8	0.014	0.192	0.187	0.586	-0.189	1.040	0.042	0.192	-72.025	0.586	-0.002	1.040
10	-0.224	0.451	-0.081	0.349	-0.189	0.768	-0.398	0.451	-72.326	0.349	0.0001	0.768
12	0.010	0.249	-0.423	0.916	-0.189	0.299	0.209	0.249	-74.207	0.916	-0.003	0.299
17	-0.280	0.202	-4.974	0.401	-0.193	0.302	-3.623	0.202	-88.033	0.401	-0.0003	0.302

From the results of running No. 1, 2 and 3 shows that the offloading system has very good behavior in 180^0 incident waves. Also, in 270^0 incoming waves both FPSO and LNG Shuttle tanker have good behavior in long wave (Run No. 5). While, in the short waves (Run No. 5 and 6) it has large motions of surge and sway. In order to get explanation for the cause of it then it will be easier to express it in to spectrum response.

Start from analyzing the spectrum response from Run No. 4 as shown in Figure 29 below, the sway motion is laid on the very low frequency. By picking the peak value of the motion, the peak period is found equal to 214 s for FPSO and 127 s for LNG Tanker. Since the wave period is equal to 7 s, then the motion is might be resonance with the slowly varying force.

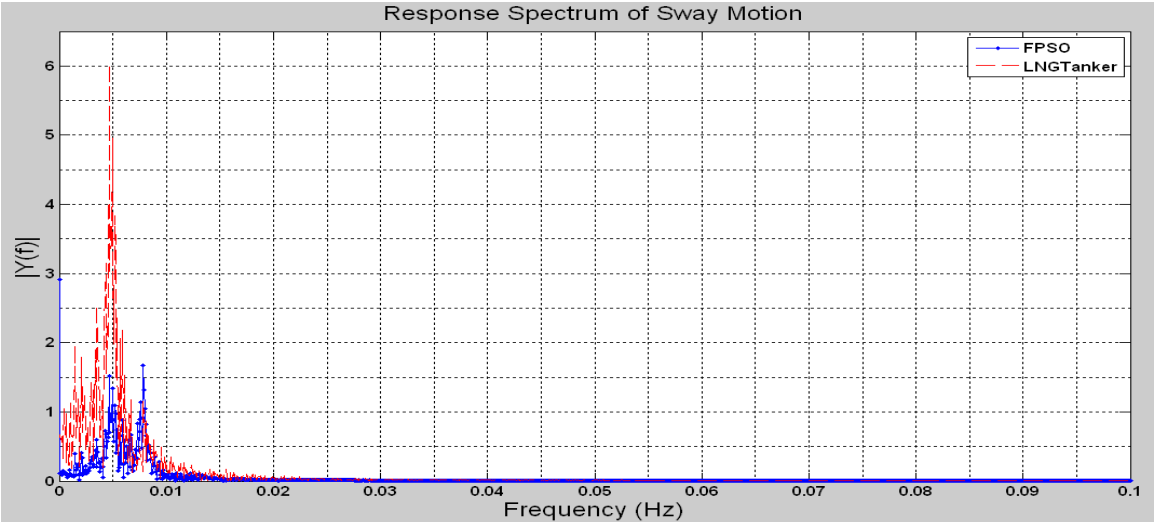

Figure 29. Sway Motion Response Spectrum from Run.No 4

Comparing with the response spectrum for running No. 5 in Figure 31, the spectrum response for running no.4 has bigger energy. In Run No.5 instead of second order forces there are also first order forces acting to the structures.

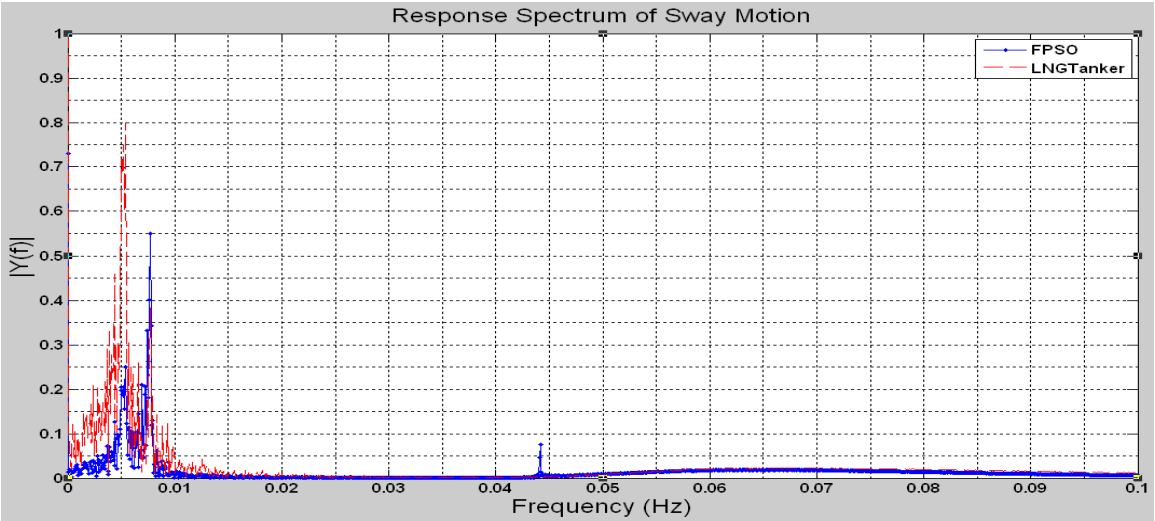

Figure 30 Sway Motion Response Spectrum from Run.No 5

Here, the hydrodynamic effect can be seen from Run No 2 and 10 for 180^0 incident waves and Run No. 5 and 12 for 270^0. From the result concluded that the hydrodynamic interaction increases the motion of the FPSO and LNG Shuttle tanker.

The time series of FPSO motion in Hs = 2m, Tp = 14 s and incident waves 270^0 is shown as Figure 31 below.

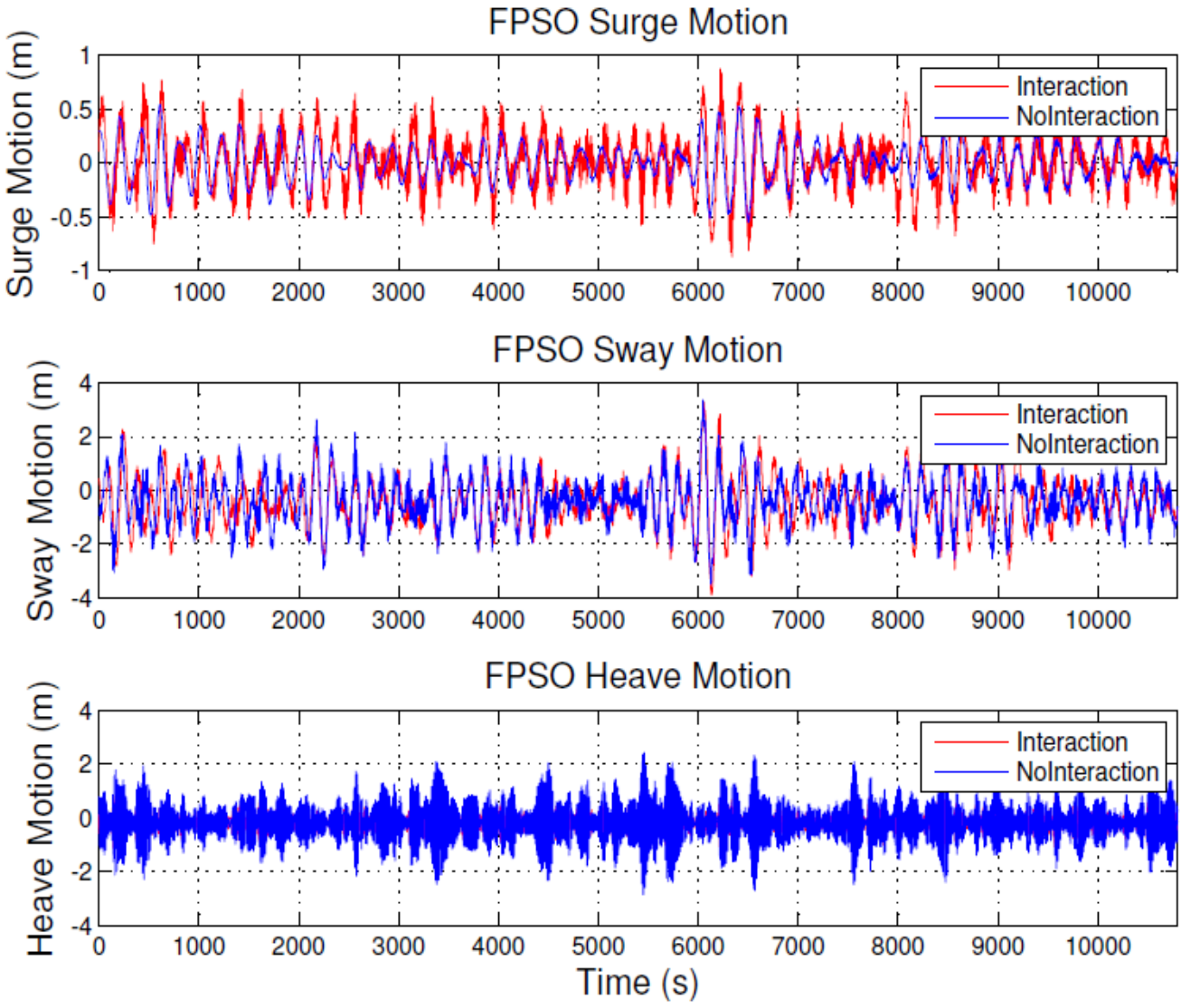

Figure 31 FPSO Motion in Hs = 2m, Tp = 14 s and 270^0 incident waves

For FPSO, the increasing motions due to the hydrodynamic influence are clearly shown from the differences between the red curve and blue curve above. In surge motion the influence is larger compare to sway and heave motions. The mean and standard deviation for surge are 0.0004 m and 0.175 m when hydrodynamic isn't considered and 0.010 m and 0.249 m when hydrodynamic interaction is considered.

For LNG Tanker, the time series of motion is shown as Figure 32 below.

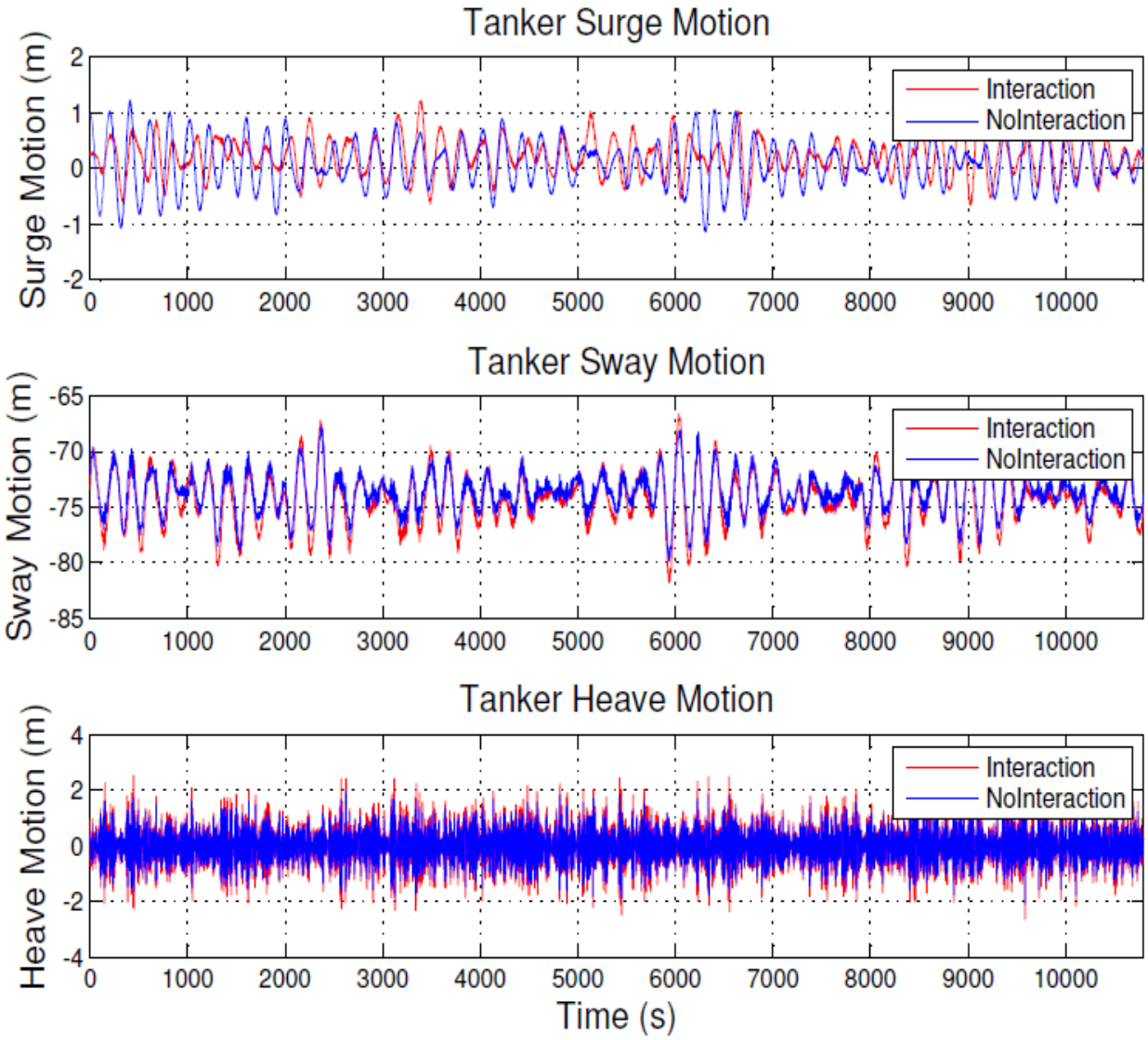

Figure 32 Tanker Motion in Hs = 2m, Tp = 14 s and 270^0 incident waves

While, for tanker motion the largest influence is occurred at sway motion. For incoming wave 270^0 there is also shielding wave from the FPSO acting to the LNG Shuttle tanker.

The effect of wind and current in FPSO and LNG Shuttle Tanker can be observed from motion time series in Figure 33 and Figure 34 respectively.

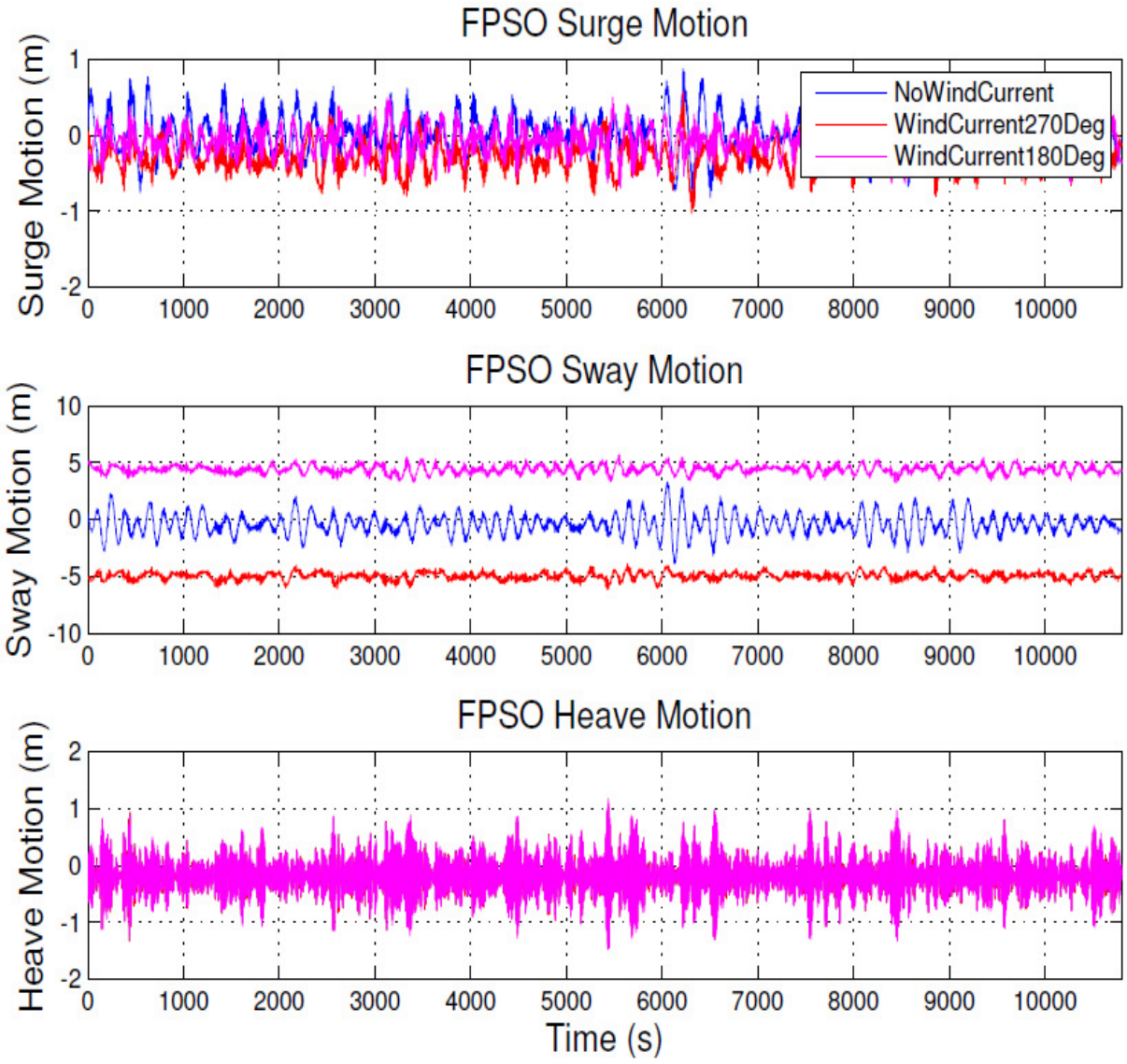

Figure 33 FPSO Motion in Hs = 2m, Tp = 14 s and 270^0 incident waves include 10 m/s Wind and 1 m/s Current

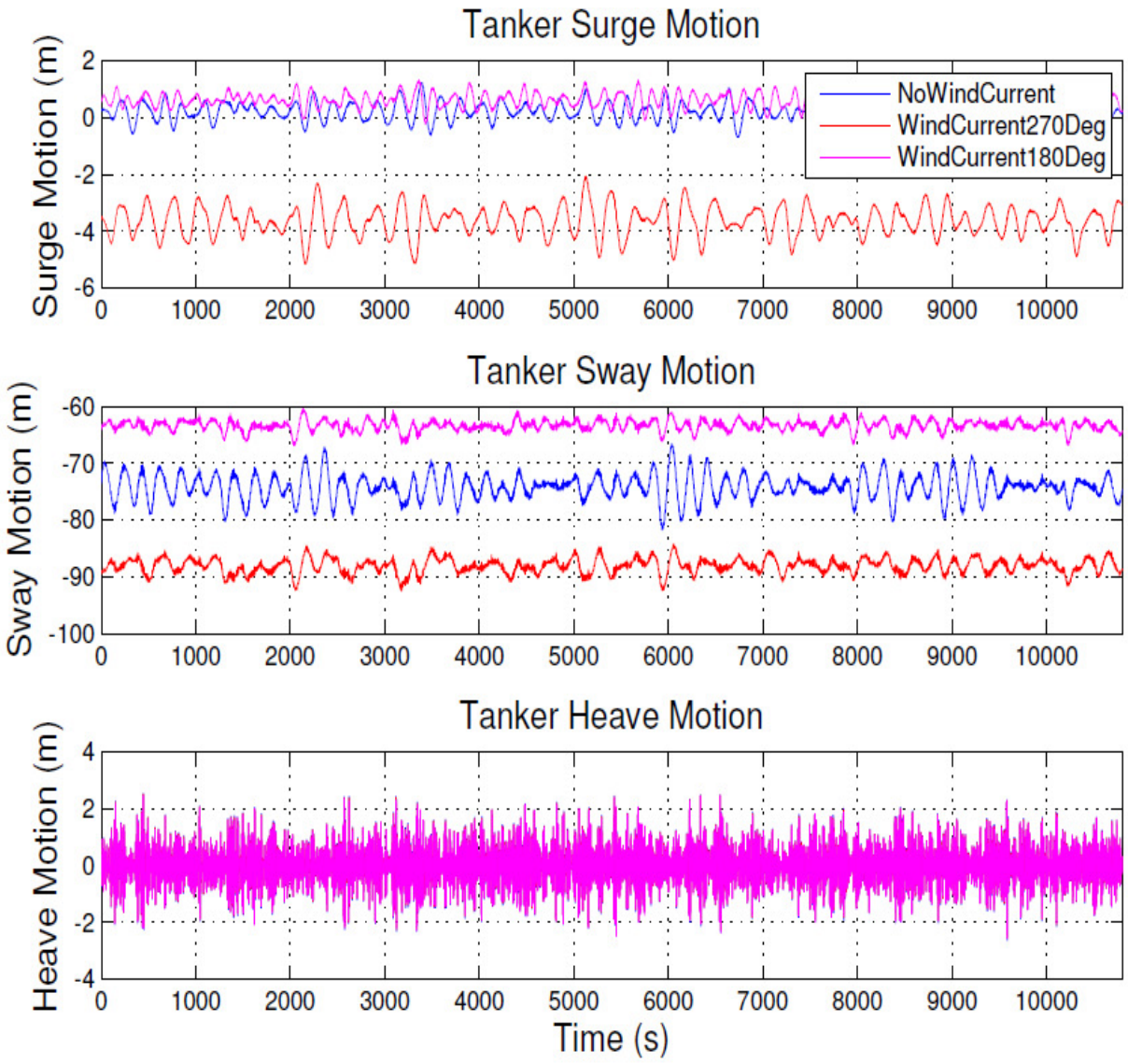

Figure 34 Tanker Motion in Hs = 2m, Tp = 14 s and 270^0 incident waves include 10 m/s Wind and 1 m/s Current

From Figure 33 and Figure 34 the conclusion is that wind and current has significant effect to the offloading system in long waves. The biggest motion will reached when wind, current and waves generates in the same direction.

CHAPTER VII MOORING ANALYSIS

The aim of the mooring analysis presented in this chapter is to ensure the mooring line has adequate capacity to restrain the offloading system motions. The mooring line tension is expressed as the statistical value of mean, standard deviation and the estimate maximum value. The statistical calculation is done in SIMO. Further, the mooring analysis is done by taking the estimate 3 hour maximum value multiplied by the API safety factor and divided by the Maximum Breaking Load of each mooring line[35].

7.1. Mooring Tension

The result for six running conditions is summarized as Table 15 below.

Table 15 Mooring Line Tensions

Run No.	Highest Line	Mean [kN]	Std Dev.[kN}	Est. 3 Hor Max. Value [kN]	1.67 x 3 Hour Max. MBL Use [%}
1	FPSO Line9	1984	10.57	2021	56.3
	L3	734	24.18	822.7	50.5
	L4	747	28.20	829.4	50.9
	Tanker Line1	194	10.00	228.8	19.1
	Tanker Line2	179.2	11.10	206.1	17.2
	L5f	362	24.67	430.9	36.0
	L5fa	376.8	24.90	468.2	39.1
	LBuoy	742.5	27.60	816.8	68.2
2	FPSO Line12	1991	15.4	2060	57.3
	L3	734	39.37	911.1	55.9
	L4	748	39.53	885.7	54.4
	Tanker Line1	193.2	11.89	238.0	19.9
	Tanker Line2	180	11.8	219.2	18.3
	L5f	362.4	26.14	449.6	37.5
	L5fa	377.1	27.18	470.3	39.3
	LBuoy	743.1	16.64	800.1	66.8

Run No.	Highest Line	Mean [kN]	Std Dev.[kN}	Est. 3 Hor Max. Value [kN]	1.67 X 3 Hour Max. MBL Use [%]
5	FPSO Line11	2022	79.40	2304	64.1
	L3	800.5	91.25	1142	70.1
	L4	803.8	106.4	1186	72.8
	Tanker Line1	171.6	16.63	254.4	21.2
	Tanker Line2	172.9	20.72	262.3	21.9
	L5f	330	56.9	523.3	43.7
	L5fa	318.0	59.95	547.1	45.7
	LBuoy	652.6	114.1	1065	88.9
12	FPSO Line12	2026	79.05	2378	66.2
	L3	827.2	113.8	1280	78.6
	L4	829.5	111.8	1278	78.5
	Tanker Line1	167.1	20.48	271.9	22.7
	Tanker Line2	169.2	22.20	280.2	23.4
	L5f	318.5	59.93	530.3	44.3
	L5fa	299.6	80.36	621.6	51.9
	LBuoy	623.0	136.3	1131	94.4
18	FPSO Line11	2495	51.26	2794	77.8
	L3	1414	88.98	1828	112.2
	L4	1344	78.11	1679	103.1
	Tanker Line1	106.1	5.197	184.8	15.4
	Tanker Line2	97.88	4.82	184.8	15.4
	L5f	10.3	14.52	385.4	32.2
	L5fa	139.6	27.65	385.4	32.2
	LBuoy	161.3	33.02	773.6	64.6

From Table 15 running no. 2, 5 and 12 show that the mooring system have adequate capacity in Hs = 2m, Tp = 14 and incident waves 180^0 and 270^0.

It also shows that the influence of hydrodynamic interaction will increase the mooring line tension. In running no. 5 where hydrodynamic interaction is not considered, the maximum capacity occurs in Line

buoy with percentage of MBL use is 88.9%. While In running no. 12 where the hydrodynamic interaction is included the percentage of MBL use in Line buoy become 99.4%.

In running no. 18 where include the wind and current force will give significant increment in line tension. Sea-state with Hs = 2 m, Tp = 14 s combined with 10 m/s wind and 1 m/s current acting in the same direction (27^0) give coupling line (L3 and L4) exceed the line capacity. It also might by lead to slack in the back up line (L5f).

Further than, this combination of sea-state need to be noticed for the further analysis. The improvement of the mooring configuration design needs to be taken to encounter this sea-state.

CHAPTER VIII CONCLUSION

8.1. Conclusion

There are two main objectives of this study. First, to establish the offloading configuration and to study the influence of hydrodynamic interaction during offloading process. Second, to perform mooring analysis in order to ensure that mooring lines have enough capacity to keep the offloading system in specified position.

Single body and multi-body analysis in regular waves have been performed in frequency domain. The aim is to determine the hydrodynamic coefficients (given in added mass coefficient, damping coefficient, and hydrostatic restoring forces) and exciting force (given in wave frequency forces and mean drift forces transfer function) acting on the FPSO and LNG Shuttle tanker.

Further, an offloading configuration sketched at Figure 23 intended for the LNG application is selected for the analysis. Static equilibrium analysis was performed in order to get equilibrium position of the offloading system and obtained the initial tension of the mooring lines. Thereafter, decay test was performed to ensure that the offloading configuration has reasonable natural period and favorable motions.

In order to examine the offloading system performance in irregular waves, wind and current, time domain analysis was performed in 18 combinations of sea-state. The results are presented in the statistical properties, i.e. mean and standard deviation of motions (Table 14). The influence of the hydrodynamic interaction and the effect of wind and current to the offloading system are also presented in time series at Figure 31 - Figure 34.

Finally, the mooring analysis was done by comparing the 3 hour maximum tension calculate from SIMO with the Minimum Breaking Load (MBL) of the mooring lines. Here, the API safety factor of 1.67 was applied.

From the step of works described above, following conclusions are gained.

The LNG offloading system is designed in side by-side configuration with 5 m distance between FPSO and LNG Shuttle Tanker. FPSO has 12 mooring lines which attached in three points. While, the LNG Shuttle Tanker has 2 mooring lines in the bow and aft, 2 coupling line connected to FPSO, 2 back-up lines connect to the buoy and the line buoy toward to the anchor. The offloading configuration(including mooring system arrangement) described here is only the typical arrangement for the LNG offloading system. The best arrangement needs an optimization study by performing the analysis including hydrodynamic interaction for various arrangement and distance between FPSO and LNG shuttle tanker. The best arrangement should be selected based on the one which gives the lowest responses on the loading arm for given sea states under consideration. Since the focus on this thesis is the hydrodynamic interaction rather that the optimization of mooring lines than the optimization study was not performed.

From the single body and multi-body analysis in regular wave shows that the hydrodynamic interaction can be observed from added mass, potential damping and exciting forces. By considering the hydrodynamic interaction the added mass of FPSO in sway and heave are decreased in certain frequency range. While for LNG Shuttle tanker, consider the hydrodynamic interaction decreases the added mass.

Further, in FPSO Increasing potential damping occurred around the resonance frequency. While, for tanker the hydrodynamic interaction decreases the potential damping. The other influence is also occurred in wave drift. By consider it; the wave drift has both positive and negative value. In 270^0 incident wave (positive y-axes), the negative wave drift is come from the reflection wave from LNG Shuttle Tanker.

From the time domain analysis concluded that the offloading system has very good behavior both in short waves and long wave in 180^0 incoming waves. While, in 270^0 the offloading system has good behavior in long wave. In short waves, the surge and sway motion is dominated by second order forces.

The influence from hydrodynamic interaction in the offloading system in variation of sea-state was observed. In increasing sea-state, the hydrodynamic interaction endorses increasing wave frequency force. In second order force, by considering the hydrodynamic interaction will produce both positive and negative wave drift force.

In low sea-state, presence of wind and current gives small influence in global force. While, in high sea-state (Hs=2 m, Tp = 14 s), presence 10 m/s wind and 1 m/s current gives large motion in surge and sway motions.

From the mooring system analysis concludes that the mooring system has adequate capacity in Hs=2 m, Tp = 14 s and incident waves 180^0 and 270^0. While, including 10 m/s wind and 1 m/s current in sea-state above leads coupling line (L3 and L4) excess the line capacity. It also might be lead slack in back-up line (L5f). Therefore, in this variation of sea-state the mooring configuration need to be improve.

Finally, based on the explanation above we can conclude that in side-by side offloading configuration with 5 m distance the hydrodynamic interaction has significant influence on several aspects. Therefore the hydrodynamic interaction must be considered in the analysis.

8.2. Recommendation for Further Work

Author realizes that in this study all cases regarding the offloading system design and analysis could not be covered. Therefore some recommendation below is propose to continue this study.

1. Calculation of the horizontal distance from FPSO and LNG tanker based on the result from sub-chapter 6.5 in purpose of Loading arm design.
2. Fendering design.
3. Optimization study of offloading configurations in various mooring configurations and distance.

REFERENCES

1. *FPSO World Fleet. 2008; Available from: http://www.fpso.net/.*
2. *Gu, Y. and Y. Ju, LNG-FPSO: Offshore LNG solution. 2008.*
3. *Shimamura.Y, FPSO/FSO: State of the art. Marine Science and Technology, 2002.*
4. *Sevanmarine. The Sevan Technology Available from: http://www.sevanmarine.com/.*
5. *SevanMarine, Offloading and Cyclonic Conditions Study. 2007.*
6. *Journée, J.M.J. and W.W. Massie, Offshore Hydromechanics 2001: Delft University of Technology.*
7. *DNV, WADAM Users Manual, Version 8.1. 2005.*
8. *Faltinsen, O.M., Sea loads on ships and offshore structures. 1990, Cambridge ; New York: Cambridge University Press. viii, 328 p.*
9. *Newman, J.N., Marine hydrodynamics. 1977, Cambridge, Mass.: MIT Press. xiii, 402 p.*
10. *Chakrabarti, S.K., Hydrodynamics of offshore structures. 1987, Southampton ; Boston: Computational Mechanics. xvii, 440 p.*
11. *Pauw, W., R. Huijsmans, and A. Voogt, Advance in the Hydrodynamics of Side-by-Side Moored Vessels. OMAE, 2007.*
12. *Koo, B.J.K., M.H, Hydrodynamic Interactions and relative motions of two floating platforms with mooring lines in side-by-side offloading operation. 2006.*
13. *Koo, B.J.K., et.al. , Vessel/mooring/riser coupled dynamic analysis of a turret-moored FPSO compared with OTRC experiment. 2005.*
14. *Kim MH, A.M., Hull/mooring/riser coupled dynamic and sensitivity study of a tanker-based FPSO. 2003.*
15. *Fang, M.-C. and G.-R. Chen, Hydrodynamic Interactions between Two Ships advancing in waves. Taiwan, 2000.*
16. *Buncher, B., J.d. Wilde, and G.d. Boer, The Interaction Effects of Mooring in Close Proximity of Other Structures. MARIN, 2004.*
17. *Buncher, B., A.v. Dicjk, and J.d. Wilde, Numerical Multiple-Body Simultions of Side-by-Side Mooring to an FPSO. MARIN, 2001.*
18. *Bok kim, Y., Doctoral dissertation Dynamic Analysis of Multiple-Body Floating Platforms coupled with Mooring Lines and Risers, in Ocean Engineering. 2003, Texas A&M University.*

19. *Naciri, M., O. Waals, and J.d. Wilde, Time Domain Simulations of Side-by-Side Moored Vessels Lesson Learnt from a Benchmark Test. OMAE, 2007.*

20. *Huijsmans, R., J.d. Wilde, and J. Pinkster, Diffractions and Radiation of Waves Around Side-by-Side Moored Vessels. The International Society of Offshore and Polar Engineers, 2001.*

21. *Morandini, C., F. Legerstee, and J. Mombaerts, Criteria for Analysis of Offloading Operation. OTC, 2002.*

22. *Hong, e.a., Numerical and Experimental Study on Hydrodynamic Interaction of Side-by-side moored Multiple Vessels. Korea, 2004.*

23. *Hung, S.M. and R.E. Taylor, The Formulation of Mean Drift Forces and Moments. London Centre for Marine Technology.*

24. *Faltinsen, O.M. and A.E. Loken, Slow Drift Oscillations of a shp in Irregular Waves. Applied Ocean Research, 1978.*

25. *Pinkster, J.A., Mean and Low Frequency Wave Drifting Forces on Floating Structures. Ocean Engineering, 1979.* ***6****.*

26. *Hung, S.M. and R. Eatock Taylor, The Formulation of Mean Drift Forces and Moments for Floating Bodies. London Centre for Marine Technology.*

27. *Faltinsen, O.M., Wave and Current Induced Motions of Floating Production System. Elsevier, 1994.*

28. *Chakrabarti, S.K. and Knovel (Firm). Handbook of offshore engineering. 2005; 2 v. (xx, 1278 p.)]. Available from: http://www.knovel.com/knovel2/Toc.jsp?BookID=1660 MIT Access Only.*

29. *MARINTEK, SIMO - Theory Manual. 2008, Trondheim.*

30. *SwarthmoreCollege. Convolution. Available from: http://www.swarthmore.edu/NatSci/echeeve1/Ref/Convolution/Convolution.html.*

31. *MARINTEK, MIMOSA - User's Documentation. 2003, Trondheim.*

32. *Van den Boom, H.J.J., Dynamic Behaviour of Mooring Lines. Maritime Research Institute Netherlands, 1985.*

33. *DNV, HydroD User Manual. 2008.*

34. *DNV, Genie User Manual. 2005.*

35. *Institude, A.P., API RP 2SK, in Design and analysis of stationkeeping systems for floating structures. - 3rd edition. 2005.*

Appendix A: SIMO Input

Appendix B: Decay test Results

Appendix C: Time Series Results